SIMULATION MODELING OF STATISTICAL NAKAGAMI-*m* FADING CHANNELS

Thesis submitted in partial fulfillment of the requirement for the award of the degree of

MASTER OF ENGINEERING (M.E.)

In

ELECTRONICS AND COMMUNICATION ENGINEERING

Submitted By

MANNAM RAMA RAO

Roll No. 800861009

Under the guidance of

Dr. AMIT KUMAR KOHLI

Assistant Professor

ECED, TU

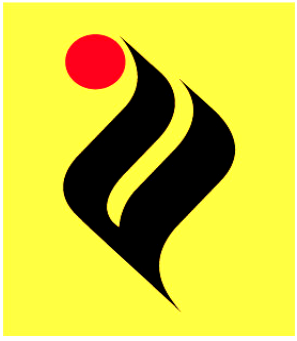

DEPARTMENT OF ELECTRONICS AND COMMUNICATION ENGINEERING

THAPAR UNIVERSITY

PATIALA-147004, PUNJAB, INDIA,

June 2010

CERTIFICATE

I, Mannam Rama Rao, hereby declare that this report entitled *"Simulation modeling of statistical Nakagami-m fading channels"* is an authentic record of my own work carried out towards the partial fulfillment for the award of degree of M.E. (Master of Engineering) in Electronics and Communication Engineering Department, Thapar University, Patiala under the guidance of Dr. Amit Kumar Kohli, Assistant Professor, ECED, during January to June 2009.

The matter presented in this report has not been submitted by me in any other University or Institute for the award of other degree.

(Mannam Rama Rao)

Signature of student

Dated: 30/06/2010

This is certified that the above statement made by the student is correct to the best of my knowledge and belief.

(Dr. Amit Kumar Kohli)

Assistant Prof., ECED

Dated: 30/06/2010

Countersigned By:

(Dr. A. K. Chatterjee)

Head of Department, ECED

Thapar University, Patiala

Dated: 2.7.10

(Dr. R.K. Sharma) 5/7/10

Dean, Academic Affairs

Thapar University, Patiala

Dated:

ACKNOWLEDGMENT

Thesis Report is simply the culmination of a few years of learning. This learning process has been possible thanks to many people that believed in me and kept on teaching me many things about life, about science and engineering, and about learning. I express my gratitude to the Thapar University, Patiala, for giving me the opportunity to work on the report during my M.E. programme.

Firstly, I would like to thank my thesis guide **Dr Amit Kumar Kohli** (Asst. Prof., ECED), whose input has been of great significance and help for me towards the successful completion of this thesis work. I would like to thank to **Dr. A. K. Chatterjee**, Head, and Electronics and Communication Engineering department, for his kind support. I am expressing my sincere thanks to all other faculty members of EC department for their valuable suggestions.

I am immensely grateful to my family members, particularly to my parents. They have always supported me and taught me the things that matter most in life.

At last but not the least, I would like to thank everyone who had helped me knowingly and unknowingly.

Mannam Rama Rao

Mannam Rama Rao

ABSTRACT

The fading, which is caused due to multipath propagation in a communication channel, challenges the wireless communication engineer who tries to establish a reliable communication path between transmitter and receiver. The fading is especially very severe when there is no line-of-sight component, which is the most occurring case in urban and suburban cities. Generally, the multipath fading amplitude distribution is modeled with Rayleigh PDF. But when the fading is very severe, the Rayleigh model failed to characterize the exact channel characteristics. So, a powerful model, named Nakagami-*m* model, is used to represent the channel.

Many techniques like "Pätzold analytical deterministic simulation model, first-order hidden markov model" were proposed to model a communication channel with Nakagami-*m* distribution for $0 \leq m \leq 1$. In this thesis report, a more computationally efficient method is introduced which takes the advantage of product of two independent random processes, namely, a square root beta process and a complex Gaussian random process. First, the square root beta process is realized by a well known technique known as inverse PDF. Next, the complex Gaussian random process is realized with the technique "rice's sum of sinusoids", in which the required parameters are calculated with optimal approximation method given by Matthias Pätzold.

The method has been implemented with the mathematical tool MATLAB. The generated complex random process, its magnitude and phase PDF plots were drawn and compared with the actual plots. For future scope, a ready to implement simulation procedure has been suggested to apply this method to generate the correlated Nakagami-*m* fading channels using the same technique.

Key words: Nakagami-*m*, Statistical, Fading Channels, Square Root Beta Process, Wireless Channels, Correlated Channels, HF channels, Flat Fading.

TABLE OF CONTENTS

Declaration **i**

Acknowledgement **ii**

Abstract **iii**

List of figures **vii**

List of tables **ix**

List of abbreviations **ix**

CHAPTER 1 **1-7**

INTRODUCTION **1**

1.1 Introduction 1

1.2 Fading 2

1.2.1 Multi Path Fading 2

1.3 Types Of Fading 3

1.3.1 Large-Scale Fading 4

1.3.2 Small-Scale Fading 4

1.4 Motivation 5

1.5 Thesis objective 7

1.5 Thesis Organization 7

CHAPTER 2 **8-30**

FADING CHANNEL- BASICS **8**

2.1 Fading Channel- Impulse Response 8

2.2 Doppler Spectrum 9

2.3 Mobile Multipath Channel Parameters 10

2.3.1 Time Dispersion Parameters 11

2.3.2 Frequency Dispersion Parameters 13

2.3.3 Spectral Shape Due To Doppler Spread 14

2.4 Types Of Small Scale Fading 14

2.4.1 Fading Effects Due To Time Delay Spread 17
2.4.2 Fading Effects Duo To Doppler Spread 20
2.5 Stochastic Processes 22
2.5.1 Properties Of Random Processes 23
2.6 Different Types Of Random Processes 26
2.6.1 Gaussian Distribution 27
2.6.2 Rayleigh Distribution 28
2.6.3 Ricean Distribution 28
2.6.4 Beta Distribution 29
2.6.5 Gamma Distribution 30

CHAPTER 3 31-40

LITERATURE SURVEY 31

3.1 Nakagami-*m* Distribution 31
3.1.1 Statistical Properties Of Nakagami-m Distribution 32
3.1.2 Higher Order Statistics Of Nakagami-m Distribution 33
3.1.3 Relation To Other Random Variables 34
3.2 Generation Of Nakagami-*m* Processes 35
3.2.1 Generation Of Nakagami Signals For $m<1$ 35
3.2.2 Generation Of Uncorrelated Nakagami Signals 36
3.2.3 Generation Of Correlated Nakagami Signals 37

CHAPTER 4 41-55

FADING CHANNEL- STATISTICAL MODELS 41

4.1 Different Fading Models 41
4.1.1 Rayleigh Fading Model 42
4.1.2 Ricean Fading Model 45
4.2 Nakagami-*m* Fading Model 46
4.3 Problem Formulation 47

4.3.1 Modeling Of Single Channel 47
4.3.2 Modeling Of Correlated Diversity Channels 49
4.3.3 Generation Of Square Root Beta Process 51
4.3.4 Generation Of WSS Complex Gaussian Process 52
CHAPTER 5 **56-60**
SIMULATION AND RESULTS **56**
5.1 Simulation Steps 56
5.1.1 Details of parameters, schemes and values used 59
5.2 Results And Analysis 60

CHAPTER 6 **69**
CONCLUSION AND FUTURE SCOPE **69**
6.1 Conclusion 69
6.2 Future scope 70
REFERENCES **71-73**

LIST OF FIGURES

Figure No.	TITLE	Page No.
1.1	Multi path fading channel	2
1.2	Types of multi path fading	3
1.3	Large scale& small scale fading	4
2.1	Time varying discrete-time impulse response model	8
2.2	Illustration of Doppler effect	9
2.3	Typical power delay profile with parameters	11
2.4	Doppler power spectrum for an unmodulated carrier	14
2.5	Flat fading channel characteristics	18
2.6	Frequency selective fading channel characteristics	19
2.7	Type of fading experienced by a signal as a function of T_s and B_s	21
2.8	Types of random processes	22
2.9	PDF and CDF of a Gaussian random variable with m = 3 and σ = 2	27
2.10	PDF and CDF of a Rayleigh random variable, σ^2 = 1/2	28
2.11	PDF and CDF of a Ricean random variable	29
2.12	PDF and CDF of a Beta distribution	29
2.13	PDF and CDF of a Gamma distribution	30
3.1	PDF and CDF of a Nakagami-*m* distribution	32
4.1	A typical Rayleigh fading envelope at 900 MHz	43
4.2	Rayleigh PDF	43

Figure No.	TITLE	Page No.
4.3	Phasor diagram of Rayleigh fading envelope	44
4.4	A typical Ricean fading envelope at 900 MHz	45
4.5	PDF of Ricean distributions	45
4.6	Phasor diagram of Rician fading envelope	46
4.7	Analytical models for generation of complex Gaussian process $\mu(t)$	52
4.8	Deterministic simulation models for complex GRP with given jakes PSD	54
5.1	Flow chart of simulation process	59
5.2.1	Nakagami-*m* envelop PDF for *m*=1, Ω=1	60
5.2.2	Nakagami-*m* envelop PDF for *m*=0.8, Ω=1	61
5.2.3	Nakagami-*m* envelop PDF for *m*=0.5, Ω=1	62
5.2.4	Comparison of Nakagami-*m* envelope PDFs for *m*=0.5, 0.8 &1, Ω=1	63
5.2.5	Nakagami-*m* phase PDF for *m*=1, Ω=1	64
5.2.6	Nakagami-*m* phase PDF for *m*=0.8, Ω=1	64
5.2.7	Nakagami-*m* phase PDF for *m*=0.5, Ω=1	65
5.2.8	Comparison of Nakagami-*m* phase PDFs for *m*=0.5, 0.8 &1, Ω=1	65
5.2.9	Simulated Nakagami-*m* random process for *m*=1, Ω=1	66
5.2.10	Simulated Nakagami-*m* random process for *m*=0.8, Ω=1	66
5.2.11	Simulated Nakagami-*m* random process for *m*=0.5, Ω=1	67
5.2.12	Auto correlation function of the Nakagami-*m* distribution for *m*=1	67
5.2.13	Comparison of Nakagami-*m* envelope PDFs for *m*=1, Ω=1, 5& 10	68

LIST OF TABLES

Table No.	TITLE	Page No.
2.1	Types of small scale fading	16
4.1	Types of fading models	42
5.1	$R_\mu(\Delta t)/R_\mu(0)$ values against $\rho(\Delta t)$ for 0.5 ≤ m < 1	58

LIST OF ABBREVIATIONS

AWGN	Additive White Gaussian Noise
ACF	Auto Correlation Function
ADF	Average Duration of Fades
BW	Band Width
CDF	Cumulative Distribution Function
dB	decibel
ERP	Ergodic Random Process
GRP	Gaussian Random Process
GSM	Global System for Mobile Communications
ICC	International Conference on Communications
IEEE	Institute of Electrical and Electronic Engineers
ISI	Inter Symbol Interference
LCR	Level Crossing Rate
MATLAB	Matrix Laboratory
PDF	Probability Density Function
PSD	Power Spectral Density
SD	Standard Deviation
VTC	Vehicular Technology Society
WSSRP	Wide Sense Stationary Random Process

CHAPTER 1
INTRODUCTION

In this chapter the concept of fading and different types of fading were introduced. The objective of thesis report has also been given in this chapter.

1.1 Introduction

Radio technologies have undergone increasingly rapid evolutionary changes in the recent past. As technology progresses to take advantages of more complex channel characteristics, the channel modeling required to emulate the radio environment for testing becomes both more critical and more complex. For instance, when bandwidths are increased (to Support higher data rates) receivers become more susceptible to Inter-Symbol Interference (ISI). To ensure that measurements in the lab accurately correlate to the Quality of the user's experience, channel models must account for all the aspects of the practical radio environment.

Multipath fading occurs in any environment where there is multipath propagation and there is some movement of elements, within the radio communications system. This may include the radio transmitter or receiver position, or in the elements that give rise to the reflections. The multipath fading can often be relatively deep, i.e. the signals fade completely away, whereas at other times the fading may not cause the signal to fall below a useable strength.

The fading channel is modeled with Nakagami-m distribution if the fading is severe compared to the Rayleigh distribution model. Of course, the Rayleigh distribution is a special case of Nakagami-m when m=1.

In multi path channels, small scale fading is the main issue to concentrate for communication engineer. Due to this small scale fading, the signal strength gets rapid changes over a small travel distance.

The type of fading experienced by a signal propagating through a mobile radio channel depends on the nature of transmitted signal with respect to characteristics of the channel. For HF ionospheric channel, Rayleigh distribution approximates the short-term fading statistics. But, if the variations in HF channel are high, then the simple Rayleigh model is unfit to characterize the channel, where we should to use the Nakagami-m model($0.5 \leq m < 1$).

1.2 Fading

The most troublesome and frustrating problem in receiving radio signals is variations in signal strength, most commonly known as 'Fading'. There are several conditions that can produce fading. When a radio wave is refracted by the ionosphere or reflected from the Earth's surface, random changes in the polarization of the wave may occur. Vertically and horizontally mounted receiving antennas are designed to receive vertically and horizontally polarized waves, respectively. Therefore, changes in polarization cause changes in the received signal level because of the inability of the antenna to receive polarization changes. Fading also results from absorption of the RF energy in the ionosphere. Absorption fading occurs for a longer period than other types of fading, since absorption takes place slowly. Usually, however, fading on ionospheric circuits is mainly a result of multipath propagation.

1.2.1 Multi path fading

Multipath fading is a feature that needs to be taken into account when designing or developing a radio communications system. In any terrestrial radio communications system, the signal will reach the receiver not only via the direct path, but also as a result of reflections from objects such as buildings, hills, ground, water, etc that are adjacent to the main path as shown below.

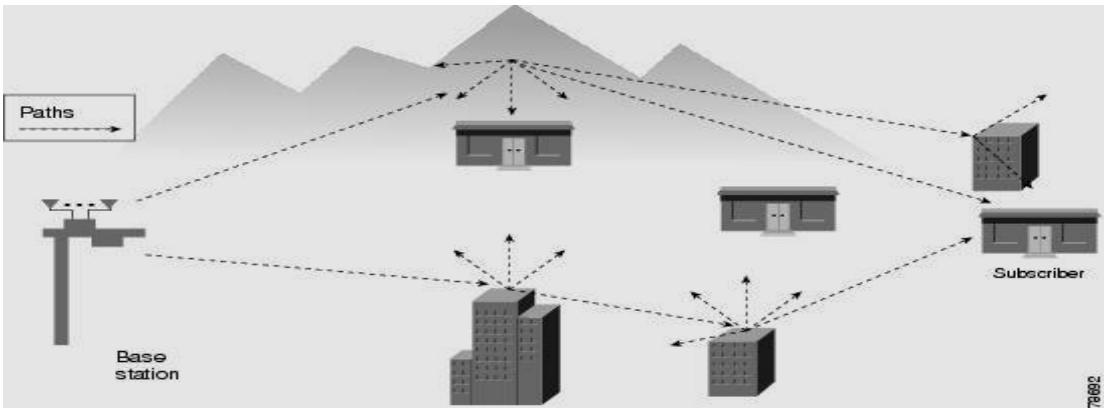

Figure 1.1: Multi path fading channel [26]

The overall signal at the radio receiver is a summation of the variety of signals being received. As they all have different path lengths, the signals will add and subtract from the total dependent upon their relative phases.

At times there will be changes in the relative path lengths. This could result from either the radio transmitter or receiver moving, or any of the objects that provides a reflective surface moving. This will result in the phases of the signals arriving at the receiver changing, and in turn this will result in the signal strength varying as a result of the different way in which the signals will sum together. It is this that causes the fading that is present on many signals. This can cause problems with phase distortion and Inter symbol interference (ISI) when data transmissions are made. As a result, it may be necessary to incorporate features within the radio communications system that enables the effects of these problems to be minimized.

1.3 Types of multi path fading

Propagation models have traditionally focused on predicting the average received signal strength at a given distance from the transmitter, as well as the variability of the signal strength in close spatial proximity to a particular location. Depends upon it, the multi path fading is mainly classified into 2 types.

A. Large scale fading
B. Small scale fading

The fallowing figure shows the complete classification of small scale and large scale fading types.

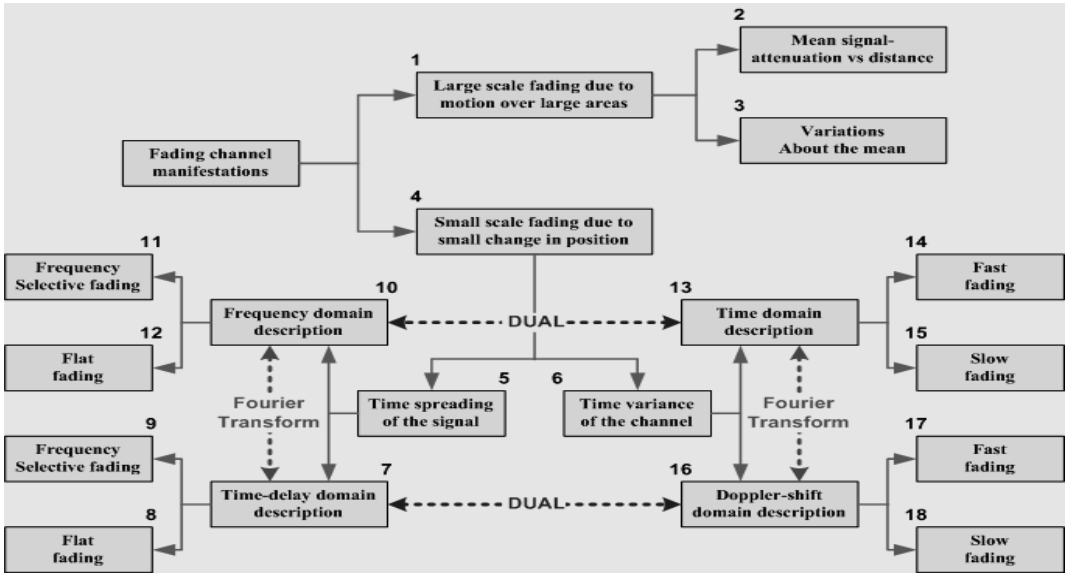

Figure 1.2: Types of multi path fading

1.3.1 Large-Scale Fading

Fading, that concentrates on the *mean* signal strength for an arbitrary transmitter-receiver (T-R) separation distance is useful in estimating the radio coverage area of a transmitter and is called large scale fading. It is mainly due to the absorption of RF energy in the ionosphere and is calculate by keeping the transmitter and receiver in the fixed positions. That's why; it is also referred to as absorption fading. The absorption occurs due to 3 types of mechanisms. They are Reflection, Diffraction and Scattering.

Different fading models are developed to estimate this large scale fading such as Longley-rice model, Durkin's model, Okumura model, Hata model, Ericsson multiple breakpoint models, Walfish and Bertoni model, etc…

1.3.2 Small - Scale Fading

Small-scale fading refers to the dramatic changes in signal amplitude and phase that can be experienced as a result of small changes (as small as half wavelength) in the spatial position between transmitter and receiver. The type of fading experienced by a signal propagating through a mobile radio channel depends on the nature of the transmitted signal with respect to the characteristics of the channel.

The fig 1.3 illustrates the relation between small scale and large scale fading.

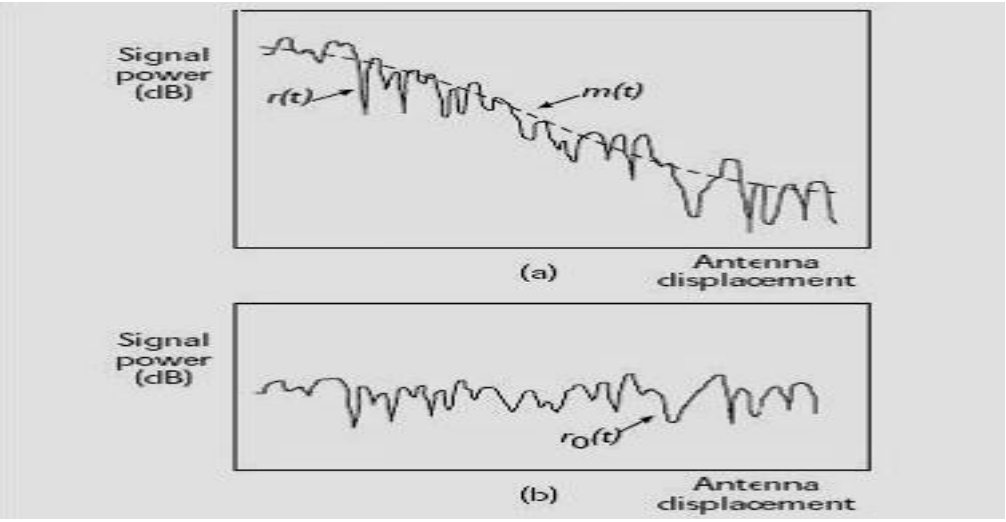

Figure 1.3: Large scale& small scale fading [5]

In fig 1.3(a), Small scale fading is superimposed on large scale fading can be easily identified. In fig 1.3(b) large scale fading m(t) has been removed in order to view the small scale fading $r_o(t)$.

Depending on the impulse response model of the fading channel, small scale fading can be divided into 4 types named as flat fading, frequency selective fading, fast fading and slow fading. Out of these, flat fading offers severe fading situation where as frequency selective fading causes the signal distortion. The different fading types were explained in this report work.

The small scale fading occurring in the multipath channel statistically obeys the different characteristics of different random processes such as Rayleigh, Rice and Nakagami-*m*, etc., these different models were discussed in this report work.

1.4 Motivation

In the recent years, radio-engineering requirements have become more stringent and necessitate not only more detailed information on median signal intensity, but also much more exact knowledge on fading statistics in both ionospheric and tropospheric modes of propagation. Such circumstances demanded a large number of experiments and number of theoretical investigations to be performed. Field tests in a mobile environment are considerably more expensive and may require permission regulatory authorities. It is difficult to generate repeatable field test results due to random, uncontrollable nature of the mobile communication path. Atmospheric conditions and cost also play a key role in field test measurements. These limitations can be overcome by means of simulation.

A simulation is an imitation of some real phenomenon, state of affairs, or process. The act of simulating generally entails representing certain key characteristics or behaviors of a selected physical or abstract system. Simulation is used in many contexts, including the modeling of natural systems or human systems in order to gain insights into their functioning. Other contexts include simulation of technology for performance optimization. Simulation can be used to show eventual real effects of alternate conditions and courses of action.

Key issues in simulation include acquisition of valid source information about the referent, selection of key characteristics and behaviors, the use of simplifying approximations and assumptions within the simulation, and the fidelity and validity of simulations results.

The main motive to run simulations can be described

- Simulation as a technique: - Investigate the detailed dynamics of a system
- Simulation as a heuristic tool: - Develop hypothesis, models and theories.
- Simulation as a substitute for an experiment: - Perform numerical experiments
- Simulation as pedagogical tool: - Gain understanding of a process.

Approximations and assumptions are used extensively to simplify the simulation model. The most commonly used assumptions and approximations involve time invariance (stationarity) and linearization. While most practical systems, when observed over a long period of time and over a wide dynamic range of input signal, might exhibit time-varying and non-linear behavior. However they can be well approximated by linear and time-invariant models over short time intervals and for low signal levels [27].

Mobile radio channel simulators thus, are essential for repeatable systems tests in the development, design or test laboratory. The Rayleigh or Nakagami fading simulator can be used to test the performance of radios in a mobile environment in the lab, without the need to perform measurements whilst actually mobile. The mobile fading simulation can also be if required be replicated, and the effects can be varied according to the 'velocity' of the mobile receiver. This allows the comparison of the performance of different receivers under standardized conditions that would not normally be possible in actual mobile testing situations. In case of mobile radio channel simulator, important assumption is time invariance. It implies that over the simulation interval, system components and properties of signal do not change.

Network Fading Simulator can also be used for the performance analysis of different modulation-demodulation schemes. Typically random binary sequences are generated and modulated using the desired modulation schemes (e.g. QPSK, PSK etc). This binary sequence is then detected under the presence of additive white Gaussian noise and multiplication noise. This multiplicative noise typically has Rayleigh or Nakagami distribution and can be generated by network fading simulator. Thus, a plot of Bit Error Rate (BER) and signal to noise ratio (S/N) can be obtained. This plot can be used to demonstrate well-known effect called flooring.

1.5 Thesis objective

In this work, an attempt has done to implement a better method, compared to already existing methods like "Pätzold analytical deterministic simulation model, first-order hidden markov model", to generate a *complex random process* that fits a given Doppler power spectrum where the amplitude fallows a *m*-distribution with *m*<1.The research work showed that this complex random process can be expressed as a product of a complex Gaussian process *w (t)* and a square-root-beta process *μ (t)* i.e.,

$$Z(t) = \mu(t)\, w(t) \tag{1.1}$$

Further, *μ (t)* can be realized by a nonlinear transformation of a Gaussian random process as given below.

$$\mu(t) = F^{-1}(\emptyset(y(t))) \tag{1.2}$$

where *y (t)* is a zero-mean unit-variance Gaussian process. ∅(.) is the CDF of ZMGRP transformation applied to *y(t)*.

When the antenna spacing is inadequate, nonindependent fading among diversity branches occurs so that the fading channels used for modeling the diversity channels are correlated. So, an attempt is made to extend the work to simulate the correlated diversity channels, too.

1.6 Thesis organization

The remaining chapters were organized as follows:

Chapter 2 introduces basic mechanisms of fading, its types, concept of random process, its properties and different types of random processes.

Chapter 3 introduces the concept of Nakagami-*m* process, its statistical properties, and the techniques available for its generation that are available in literature.

Chapter 4 explains the different statistical models like Rayleigh, Ricean and Nakagami-*m*. A procedure has been given for the generation of Nakagami-*m* random processes for both correlated and uncorrelated channels.

Chapter 5 presents the simulation steps to fallow and a thorough analysis on simulation results.

Chapter 6 gives the conclusion and future scope of this report work.

CHAPTER 2

FADING CHANNEL-BASICS

This chapter introduces the impulse response of the fading channels and its Doppler spectrum. Different types of small scale fading are thoroughly discussed in this chapter. The concept of stochastic process and important types of processes used to model the fading channels were also been introduced.

2.1 Fading Channel- Impulse Response

The small variations of a mobile radio signal can be directly related to the impulse response of the mobile radio channel. The impulse response is a wideband channel characterization and contains all information necessary to simulate or analyze any type of radio transmission through the channel. This stems from the fact that a mobile radio channel may be modeled as a linear filter with a time varying impulse response, where the time variation is due to receiver motion in space. The filtering nature of the channel is caused by the summation of amplitudes and delays of the multiple arriving waves at any instant of time. The impulse response is a useful characterization of the channel, since it may be used to predict and compare the performance of many different mobile communication systems and transmission bandwidths for a particular mobile channel condition.

The fallowing figure represents a typical time varying discrete-time impulse response model for a multipath radio channel.

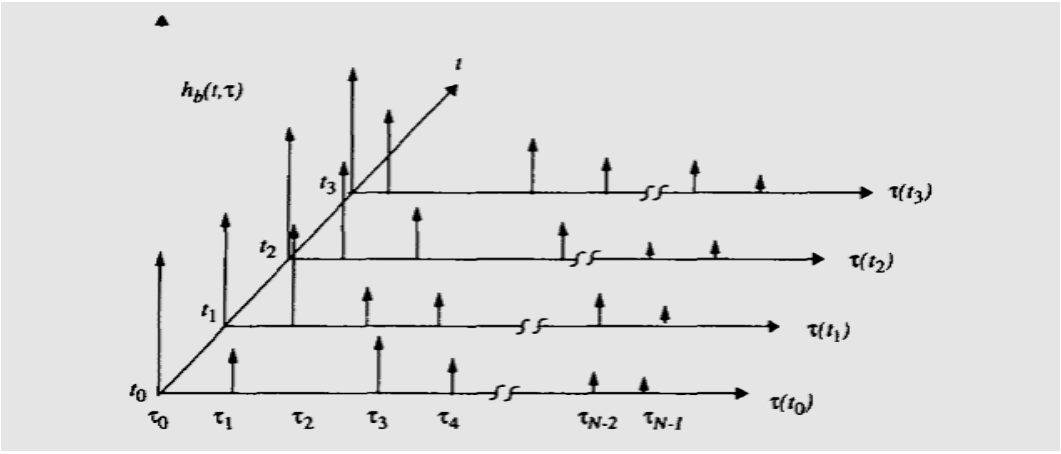

Figure 2.1: Time varying discrete-time impulse response model [5]

From this figure, the impulse response $h_b(t,\tau)$ can be found with the equation:

$$h_b(t,\tau) = \sum_{i=0}^{N-1} a_i(t,\tau)\, e^{[j\,(2\pi f_c \tau_i(t) + \emptyset_i(t,\tau))]}\, \delta(\tau - \tau_i(t)) \qquad (2.1)$$

where $a_i(t,\tau)$and $\tau_i(t)$ are the real amplitudes and excess delays , respectively, of *i*th multi path component at time t. The phase term $2\pi f_c \tau_i(t) + \emptyset_i(t,\tau)$ represents the phase shift due to free space propagation of the *i* th multipath component, plus any additional phase shifts which are encountered in the channel.

For small-scale channel modeling, the power delay profile of the channel found by taking the special average $|h_b(t,\tau)|^2$ over a local area. The received power delay profile in a local area is given by

$$P(\tau) = \overline{k|h_b(t;\tau)|^2} \qquad (2.2)$$

where the bar represents the average over local area and many snapshots of $|h_b(t;\tau)|^2$ are typically averaged over a local (small-scale) area to provide time-invariant multipath power delay profile $P(\tau)$. The gain k relates the transmitted power in the probing pulse *p(t)* to the total power received in a multipath delay profile.

2.2 Doppler spectrum

The shift in received signal frequency due to motion is called the Doppler shift, and is directly proportional to the velocity and direction of motion of the mobile with respect to the direction of arrival of the received wave. Consider a mobile moving at a constant velocity v, along a path segment having length d between points X and Y, while it receives signals from a remote source S, as shown in figure.

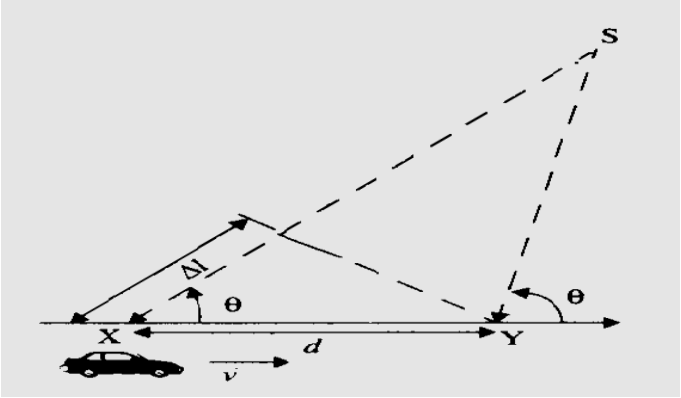

Figure 2.2: Illustration of Doppler Effect [5]

The difference in path lengths travelled by the wave from source S to the mobile at points X and Y is $\Delta l = d cos\theta = v\Delta t cos\theta$, where Δt is the time required for the mobile to travel from the X to Y, and θ is assumed to be the same at points X and Y since the source is assumed to be very far away. The phase angle in the received signal due to the difference in the path lengths is therefore

$$\Delta\emptyset = \frac{2\pi\Delta l}{\lambda} = \frac{2\pi v\Delta t}{\lambda} cos\theta \quad (2.3)$$

and hence the apparent change in frequency, or Doppler shift, is given by f_d, where

$$f_d = \frac{1}{2\pi}\frac{\Delta\phi}{\Delta t} = \frac{v}{\lambda}\cos\theta \quad (2.4)$$

From the above equation, it is clear that if the mobile is moving towards the direction of the arrival of the wave, the Doppler shift is positive (i.e., the apparent received frequency is increased), otherwise it is negative.

In a communication channel, different multipath components arrive towards receiver in different directions, which causes individual multipath components can undergo different Doppler shifts, results the Doppler spectrum. The PSD for Jakes spectrum is a commonly used method of simulating Doppler shift. It assumes that there are equal energy signals coming in all directions and as a result for a stationary transmitter and a receiver moving at a fixed speed, there will be some energy at all possible Doppler shifts from $-f_d$ to $+f_d$, with no energy at Doppler shifts outside that.

2.3 Mobile multipath channel parameters

In order to compare different multipath channels and to develop some design methods for mobile communication systems, different parameters which grossly quantify the channel are used. We can define these channel parameters with the help of power delay profile of the channel. Power delay profiles are generally represented as plots of received power as a function of excess delay with respect to a fixed time delay reference. The following figure shows the typical power delay profile plot determined from a large no. of closely sampled instantaneous profiles.

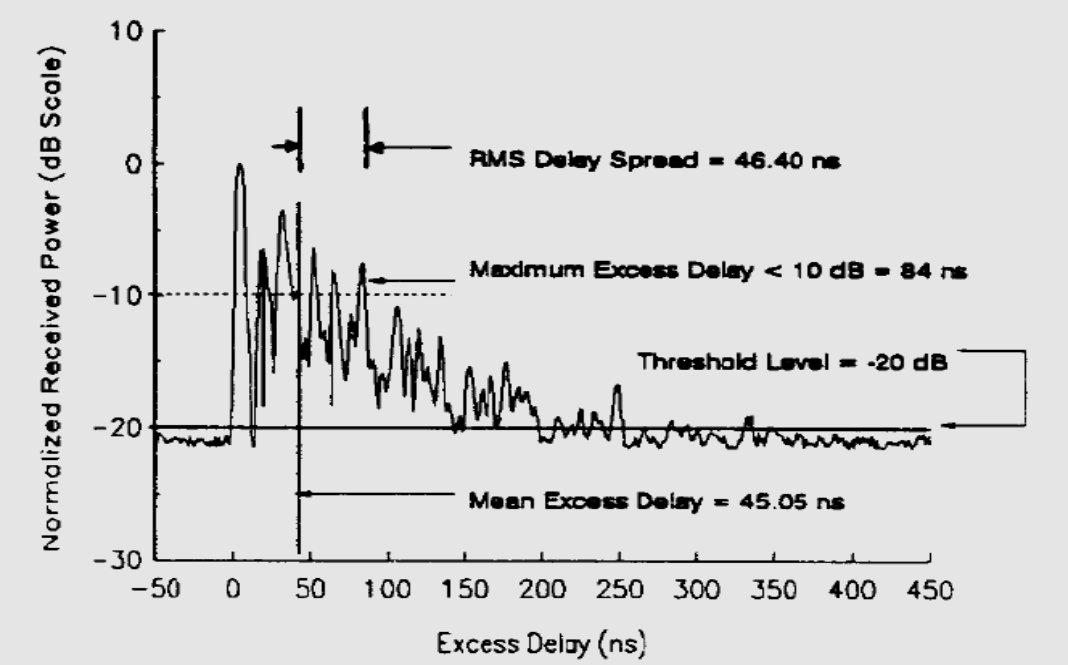

Figure 2.3: Typical power delay profile with parameters [5]

We can classify the parameters into 2 categories.

1. Time dispersion parameters
2. Frequency dispersion parameters

2.3.1 Time dispersion parameters

- Mean excess delay
- Rms delay spread
- Maximum excess delay
- Coherence bandwidth

Out of these, the first 3 parameters are time domain parameters where as the last one is the frequency domain parameter. It can be finding with the help of spectral response of the channel.

2.3.1.1 Mean excess delay ($\bar{\tau}$):

The mean excess delay is the first moment of the power delay profile defined as

$$\bar{\tau} = \frac{\sum_k a_k^2 \tau_k}{\sum_k a_k^2} = \frac{\sum_k p(\tau_k)\tau_k}{\sum_k p(\tau_k)} \tag{2.5}$$

2.3.1.2 Rms delay spread (σ_τ):

It is the square root of the second central moment of the power delay profile defined as

$$\sigma_\tau = \sqrt{\tau^2 - (\bar{\tau})^2} \tag{2.6}$$

Where

$$\bar{\tau} = \frac{\sum_k a_k^2 {\tau_k}^2}{\sum_k a_k^2} = \frac{\sum_k p(\tau_k) {\tau_k}^2}{\sum_k p(\tau_k)} \tag{2.7}$$

These 2 parameters are measured relative to the first detectable signal arriving at the receiver at $\tau_0 = 0$. These are defined from a single power delay profile which is temporal or spatial average of consecutive impulse response measurements collected and averaged over a local area.

2.3.1.3 Maximum excess delay (X dB):

The maximum excess delay (*X* dB) of a power delay profile is defined to be the time delay during which multipath energy falls to X dB below the maximum. The maximum excess delay is defined as $\tau_X - \tau_0$, where τ_X is the maximum delay at which a multipath component is within X dB of the strongest arriving multipath signal. The maximum excess delay (X dB) defines the temporal extent of the multipath that is above a particular threshold. The value of τ_X is called the excess delay spread of a power delay profile.

These parameters can be measured from the given power delay profile as shown in figure 2.3.

2.3.1.4 Coherence bandwidth (B_c):

Coherence bandwidth is the statistical measure of the range of frequencies over which the channel can be considered flat. In other words, it is the range of frequencies over which two frequency components have a strong potential for amplitude correlation. The rms delay spread and coherence bandwidths are inversely proportional to each other, mathematically given as

$$B_c \propto \frac{1}{\sigma_\tau} \tag{2.8}$$

The exact relationship between these 2 parameters is a function of specific channel impulse responses and applied signals.

2.3.2 Frequency dispersion parameters

- Doppler spread
- Coherence time

2.3.2.1 Doppler spread (B_D):

It is a measure of the spectral broadening caused by the time rate of change of the mobile channel and is defined as the range of frequencies over which the received Doppler spectrum is essentially non-zero. When a pure sinusoidal tone of frequency f_c

Is transmitted, the received signal spectrum, called the Doppler spectrum, will have components in the range f_c-f_d to f_c+f_d , where f_d is the Doppler shift. The amount of spectral broadening depends on f_d which is a function of the relative velocity of the mobile, and the angle between the direction of motion of the mobile and the direction of the arrival of the scattered waves.

2.3.2.2 Coherence time (T_c):

It is the time duration over which the channel impulse response is essentially invariant, and quantifies the channel response at different times. In other words, it is the time duration over which 2 received signals have a strong potential for amplitude correlation. This is the time domain dual of Doppler spread and is used to characterize the time varying nature of the frequency dispersiveness of the channel in the time domain.

The above 2 parameters are inversely proportional to each other given as

$$T_c \approx \frac{1}{f_m} \tag{2.9}$$

where f_m is the maximum Doppler shift.

2.3.3 Spectral shape due to Doppler spread

The spectral shape of the Doppler spread determines the time domain fading waveform and dictates the temporal correlation and fades slope behaviors. The well-known jakes PSD can be defined as

$$S_{E_Z}(f) = \frac{1.5}{\pi f_m \sqrt{1-\left[\frac{f-f_c}{f_m}\right]^2}} \tag{2.10}$$

In the above equation, the power spectral density at $f = f_c \pm f_m$ is infinite i.e., Doppler components arriving at exactly 0^0 and 180^0 have an infinite power spectral density.

The resultant jakes PSD of the unmodulated CW carrier having carrier frequency f_c is shown in the figure 2.4.

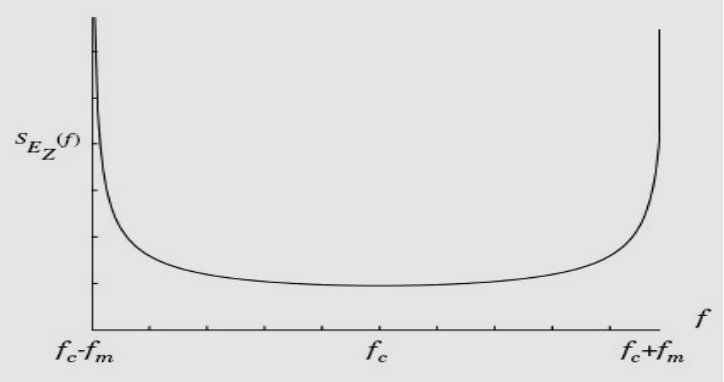

Figure 2.4: Doppler power spectrum for an unmodulated carrier [5]

2.4 Types of small scale fading

Out of 2 types of fading, the small scale fading, which generally occurs in built-up cities, is the main consideration when modeling the communication channel. The most important effects that occur due to this fading are:

1. Rapid changes in signal strength over a small travel distance or time interval.
2. Random frequency modulation due to varying Doppler shifts on different multi path signals.
3. Time dispersion (echoes) caused by multi path propagation delays.

In urban areas, fading occurs because the height of the mobile antennas is well below the height of surrounding antennas, so there is no single line of sight path to the base station. Even when light of sight exists, multipath still occurs due to reflections from the ground and surrounding structures. The incoming radio waves arrive from different directions with different propagation delays. The signal received by the mobile at any point in the space may consist of a large number of plane waves having randomly distributed amplitudes, phases, and angles of arrival. These multipath components combine vectorially at the receiver antenna, and can cause the signal received by mobile to distort or fade. Even when a receiver is stationary, the received signal may fade due to movement of surrounding objects in the radio channel.

If objects in the radio channel are static and only receiver is in motion, then fading is purely a spatial phenomenon. The spatial variations of the resultant signal are seen as temporal variations by the receiver as it moves through the multipath field. So, due to the random changes of the properties of communication channel, every communication channel is modeled with a random process which fits best for the corresponding Doppler frequency spectrum. The Doppler power spectral density of a fading channel describes how much spectral broadening it causes. This shows how a pure frequency e.g. a pure sinusoid, which is an impulse in the frequency domain, is spread out across frequency when it passes through the channel.

As discussed in chapter 1, small scale fading is the most severe problem in the design of mobile communication networks.
The physical factors those influence small-scale fading are

- Multi path propagation
- Speed of the mobile
- Speed of surrounding objects
- The transmission bandwidth of the channel

Due to the relative motion between mobile and base station, each multi path wave experiences an apparent shift in frequency which is called the Doppler shift, and it is directly proportional to the velocity and direction of motion of the mobile with respect to the direction of arrival of the received multipath wave. But due to presence of multipath components, Doppler shift experienced by individual components is different, leads to random frequency modulation.

If transmitted radio signal bandwidth is greater than the bandwidth of the multi path signal, the received signal will be distorted, but the received signal strength will not fade much over a local area. If the transmitted signal has a narrowband width as compared to the channel, the amplitude of the will change rapidly, but the signal will not distorted in time. Thus the statistics of small-scale signal strength and the likelihood of signal smearing appearing over small-scale distances are very much related to the specific amplitudes and delays of the multi path channel, as well as bandwidth of the transmitted signal.

Depending on the relation between the signal parameters (such as bandwidth, symbol period, etc.) and the channel parameters (such as rms delay spread and Doppler spread), different transmitted signals will undergo different types of fading. The time dispersion and frequency dispersion mechanisms in a mobile radio channel lead to four possible distinct effects, which are manifested depending on the nature of the transmitted signal, the channel, and the velocity. While multipath delay spread leads to *time dispersion* and *frequency selective fading*, Doppler spread leads to *frequency dispersion* and *time selective fading*. The two propagation mechanisms are independent of one another. Table 2.1 shows the types of fading.

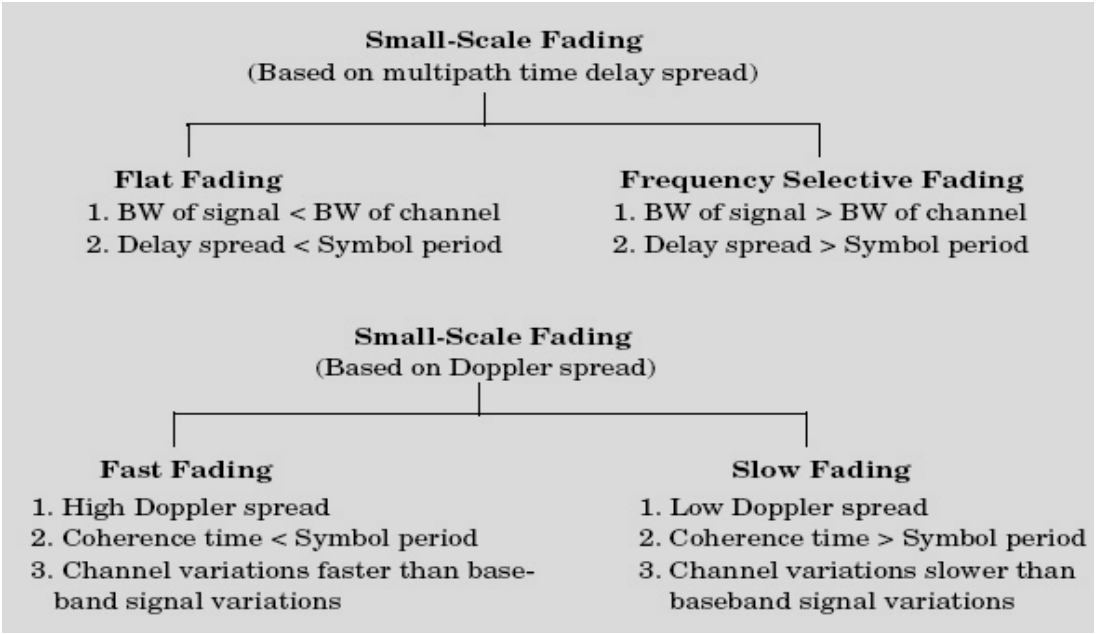

Table 2.1: Types of small scale fading [5]

2.4.1 Fading effects due to time delay spread

As discussed above, multipath time delay spread can affect *radio communications channels* and it can be classified as

- Flat fading
- Frequency selective fading

2.4.1.1 Flat fading:

If the mobile radio channel has a constant gain and linear phase response over a bandwidth which is greater than the bandwidth of the transmitted signal, then the received signal will undergo *flat fading*. In flat fading, the multipath structure of the channel is such that the spectral characteristics of the transmitted signal are preserved at the receiver. However the strength of the received signal changes with time, due to fluctuations in the gain of the channel caused by multipath.

It can be seen from Figure 2.5 that if the channel gain changes over time, a change of amplitude occurs in the received signal. Over time, the received signal $r(t)$ varies in gain, but the spectrum of the transmission is preserved. In a flat fading channel, the reciprocal bandwidth of the transmitted signal is much larger than the multipath time delay spread of the channel, and $h_b(t_\tau)$ can be approximated as having no excess delay (i.e., a single delta function with $\tau=0$).

Flat fading channels are also known as *amplitude varying channels* and are sometimes referred to as *narrowband channels*, since the bandwidth of the applied signal is *narrow* as compared to the channel flat fading bandwidth. Typical flat fading channels cause deep fades, and thus may require 20 or 30 dB more transmitter power to achieve low bit error rates during times of deep fades as compared to systems operating over non-fading channels. The distribution of the instantaneous gain of flat fading channels is important for designing radio links, and the most common amplitude distribution is the Rayleigh distribution. The Rayleigh flat fading channel model assumes that the channel induces amplitude which varies in time according to the Rayleigh distribution.

To summarize, a signal undergoes flat fading if

$$B_S << B_C \quad \text{and} \quad T_S >> \sigma_\tau \tag{2.11}$$

Where T_s is the reciprocal bandwidth (e.g., symbol period) and B_s is the bandwidth, respectively, of the transmitted modulation, and σ_τ and B_C are the rms delay spread and coherence bandwidth, respectively, of the channel.

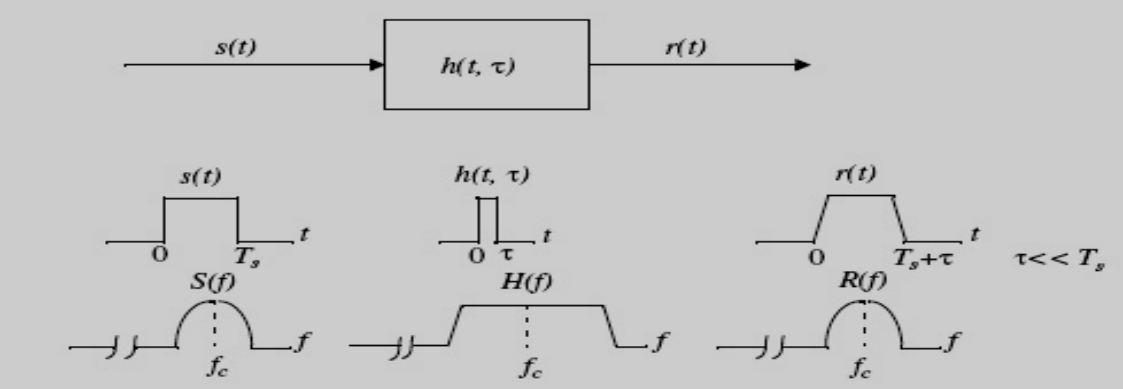

Figure 2.5: Flat fading channel characteristics [5]

2.4.1.2 Frequency Selective Fading:

If the channel possesses a constant-gain and linear phase response over a bandwidth that is smaller than the bandwidth of transmitted signal, then the channel creates *frequency selective fading* on the received signal. Under such conditions, the channel impulse response has a multipath delay spread which is greater than the reciprocal bandwidth of the transmitted message waveform. When this occurs, the received signal includes multiple versions of the transmitted waveform which are attenuated (faded) and delayed in time, and hence the received signal is distorted.

Frequency selective fading is due to time dispersion of the transmitted symbols within the channel. Thus the channel induces *inter symbol interference* (ISI). Viewed in the frequency domain, certain frequency components in the received signal spectrum have greater gains than others.

Frequency selective fading channels are much more difficult to model than flat fading channels since each multipath signal must be modeled and the channel must be considered to be a linear filter. It is for this reason that wideband multipath measurements are made, and models are developed from these measurements. When

analyzing mobile communication systems, statistical impulse response models such as the two-ray Rayleigh fading model (which considers the impulse response to be made up of two delta functions which independently fade and have sufficient time delay between them to induce frequency selective fading upon the applied signal), or computer generated or measured impulse responses, are generally used for analyzing frequency selective small-scale fading. Figure 2.6 illustrates the characteristics of a frequency selective fading channel.

For frequency selective fading, the spectrum *S(f)* of the transmitted signal has a bandwidth which is greater than the coherence bandwidth B_c of the channel. Viewed in the frequency domain, the channel becomes frequency selective, where the gain is different for different frequency components. Frequency selective fading is caused by multipath delays which approach or exceed the symbol period of the transmitted symbol. Frequency selective fading channels are also known as *wideband channels* since the bandwidth of the signal *s*(*t*) is wider than the bandwidth of the channel impulse response. As time varies, the channel varies in gain and phase across the spectrum of *s*(*t*), resulting in time varying distortion in the received signal *r*(*t*). To summarize, a signal undergoes frequency selective fading if

$$B_S > B_C \quad \text{and} \quad T_S < \sigma_\tau \,. \tag{2.12}$$

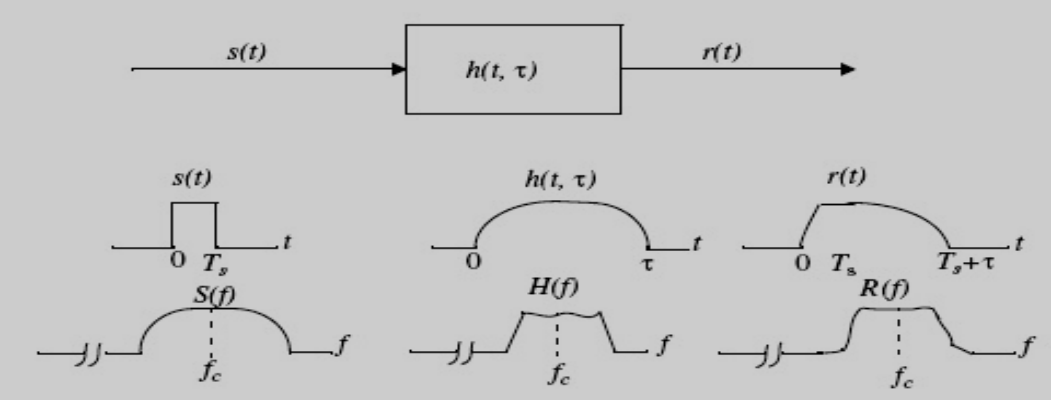

Figure 2.6: Frequency selective fading channel characteristics [5]

A common thumb rule is that a channel is flat fading if $T_S \geq 10\sigma_\tau$ and a channel is frequency selective if $T_S < 10\sigma_\tau$ although this is dependent on the specific type of modulation used.

2.4.2 Fading Effects Due to Doppler Spread

Cellular telecommunications is subject to this type of fading effects. There are a variety of reasons for this. The first is that the mobile station or user is likely to be moving, and as a result the path lengths of all the signals being received are changing. The second is that many objects around may also be moving. Automobiles and even people will cause reflections that will have a significant effect on the received signal. Accordingly multipath fading due to Doppler spread has a major bearing on cellular telecommunications. According to Doppler spread, fading can be classified as

- Fast fading
- Slow fading

2.4.2.1 Fast Fading

Depending on how rapidly the transmitted baseband signal changes as compared to the rate of change of the channel, a channel may be classified either as a *fast fading* or *slow fading* channel. In a *fast fading channel*, the channel impulse response changes rapidly within the symbol duration. That is, the coherence time of the channel is smaller than the symbol period of the transmitted signal. This causes frequency dispersion (also called time selective fading) due to Doppler spreading, which leads to signal distortion. When viewed in the frequency domain, signal distortion due to fast fading increases with increasing Doppler spread relative to the bandwidth of the transmitted signal. Therefore, a signal undergoes fast fading if

$$T_S > T_C \quad \text{and} \quad B_S < B_D \tag{2.13}$$

It should be noted that when a channel is specified as a fast or slow fading channel, it does not specify whether the channel is flat fading or frequency selective in nature. Fast fading only deals with the rate of change of the channel due to motion. In the case of the flat fading channel, we can approximate the impulse response to be simply a delta function (no time delay). Hence, a *flat fading, fast fading* channel is a channel in which the amplitude of the delta function varies faster than the rate of change of the transmitted baseband signal. In the case of a *frequency selective, fast fading* channel, the amplitudes, phases, and time delays of any one of the multipath components vary

faster than the rate of change of the transmitted signal. In practice, fast fading only occurs for very low data rates.

2.4.2.2 Slow Fading

In a *slow fading channel*, the channel impulse response changes at a rate much slower than the transmitted baseband signal *s(t)*. In this case, the channel may be assumed to be static over one or several reciprocal bandwidth intervals. In the frequency domain, this implies that the Doppler spread of the channel is much less than the bandwidth of the baseband signals. Therefore, a signal undergoes slow fading if

$$T_S << T_C \quad \text{and} \quad B_S >> B_D \tag{2.14}$$

It should be clear that the velocity of the mobile (or velocity of objects in the channel) and the baseband signaling determines whether a signal undergoes fast fading or slow fading.

The relation between the various multipath parameters and the type of fading experienced by the signal are summarized in Figure 2.7. It should to note that fast and slow fading deal with the relationship between the time rate of change in the channel and the transmitted signal, and not with propagation path loss models.

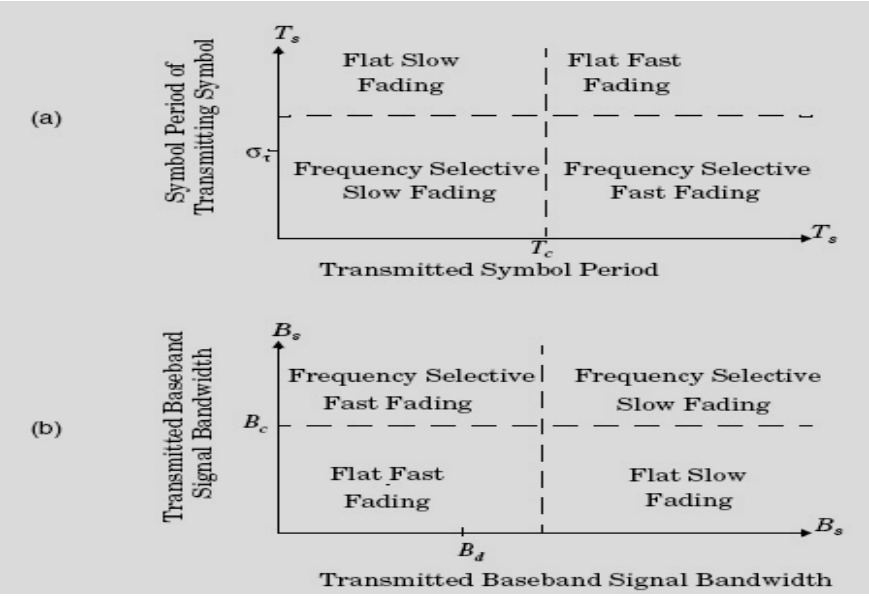

Figure 2.7 Type of fading experienced by a signal as a function of T_s and B_s [5]

2.5 Stochastic processes

A random process is a function of the elements of a sample space, *S*, as well as another independent variable, *t*. Given an experiment, *E*, with sample space, *S*, the random process, $X(t)$, maps each possible outcome, $\zeta \epsilon S$, to a function of *t*, $x(t, \zeta)$, as specified by some rule.

These random signals play a fundamental role in the fields of communications, signal processing, control systems, and many other engineering disciplines. In the study of deterministic signals, we often encounter 4 types or classes of signals:
(1) *Continuous time and continuous amplitude signals* are a function of a continuous independent variable, time. The range of the amplitude of the function is also continuous.
(2) *Continuous time and discrete amplitude signals* are a function of a continuous independent variable, time—but the amplitude is discrete.
(3) *Discrete time and continuous amplitude signals* are functions of a quantized or discrete independent time variable, while the range of amplitudes is continuous.
(4) *Discrete time and discrete amplitude signals* are functions where both the independent time variable and the amplitude are discrete.

The fallowing figure explains these different types of random processes:

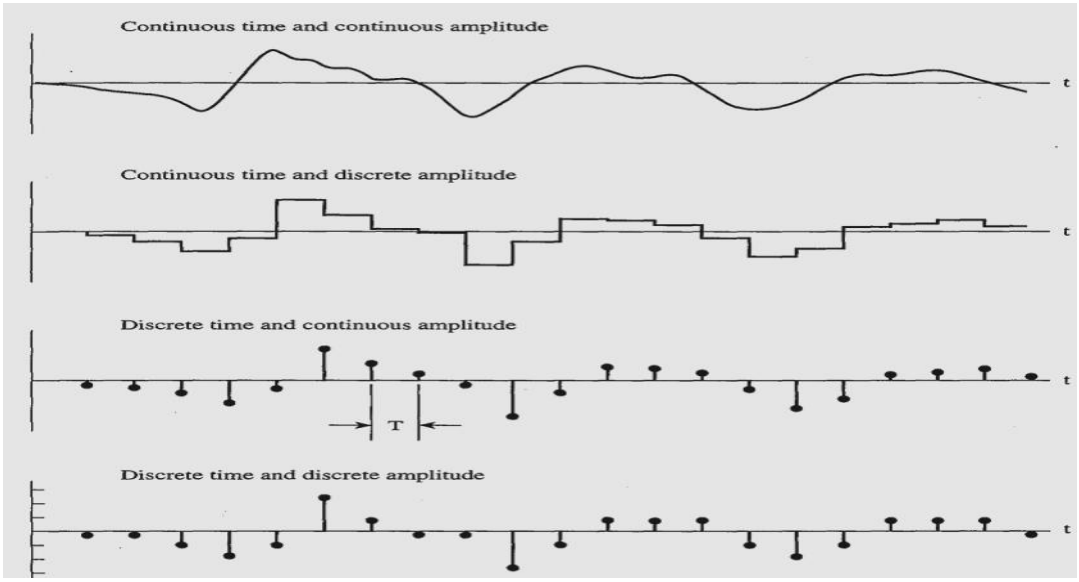

Figure 2.8: Types of Random processes [6]

A random variable, X, is a function of the possible outcomes, ζ, of an experiment. Now, we would like to extend this concept so that a function of time $x(t)$ (or $x[n]$ in the discrete time case) is assigned to every outcome, ζ, of an experiment. The function, $x(t)$, may be real or complex and it can be discrete or continuous in amplitude. Strictly speaking, the function is really a function of two variables, $x(t, \zeta)$, but to keep the notation simple, we typically do not explicitly show the dependence on the outcome, just as we have not in the case of random variables. The function $x(t)$ may have the same general dependence on time for every outcome of the experiment or each outcome could produce a completely different waveform. In general, the function $x(t)$ is a member of an *ensemble* (family, set, collection) of functions. X (t) represents the random process, while $x(t)$ is one particular member or *realization* of the random process.

2.5.1 Properties of random processes

➲ Samples of $X(t)$ at times $t_0, t_1, \ldots, t_n$ are joint random variables defined on the underlying probability space. Thus, the *joint CDF* of samples at times $t_0, t_1, \ldots, t_n$ is given by

$$P_{X(t_0)X(t_1)\ldots X(t_n)}(x_0, x_1, \ldots x_n) = p(X(t_0) \leq x_0, X(t_1) \leq x_1, \ldots, X(t_n) \leq x_n) \quad (2.15)$$

The random process $X(t)$ is fully characterized by its joint CDF $P_{X(t0)X(t1)\ldots X(tn)}(x_0, \ldots, x_n)$ for all possible sets of sample times $\{t_0, t_1, \ldots, t_n\}$.

➲ A random process $X(t)$ is *stationary* if for all T and all sets of sample times $\{t_0, \ldots, t_n\}$, we have that

$$p(X(t_0) \leq x_0, X(t_1) \leq x_1, \ldots, X(t_n) \leq x_n) = p(X(t_0 + T) \leq x_0, X(t_1 + T) \leq x_1, \ldots, X(t_n + T) \leq x_n). \quad (2.16)$$

Intuitively, a random process is stationary if time shifts do not affect its probability. Stationarity of a process is often difficult to prove since it requires checking the joint CDF of all possible sets of samples for all possible time shifts. Stationarity of a random process is often inferred from the stationarity of the source generating the process.

➲ The *mean* of a random process is defined as $E[X(t)]$. Since the mean of a stationary random process is independent of time shifts, it must be constant:

$$\mathbf{E}[X(t)] = \mathbf{E}[X(t - t)] = \mathbf{E}[X(0)] = \mu_X. \quad (2.17)$$

➲ The *autocorrelation* (ACF) of a random process is defined as

$$A_X(t, t+\tau) = \mathbf{E}[X(t)\, X(t+\tau)]. \tag{2.18}$$

The autocorrelation of $X(t)$ is also called its second moment. Since the autocorrelation of a stationary process is independent of time shifts,

$$A_X(t, t+\tau) = \mathbf{E}X(t-t)X(t+\tau-t)] = [X(0)X(\tau)] = A_X(\tau). \tag{2.19}$$

So for stationary processes, the autocorrelation depends only on the time difference τ between the samples $X(t)$ and $X(t+\tau)$ and not on the absolute time t. The autocorrelation

of a process measures the correlation between samples of the process taken at different times.

➲ Two random processes $X(t)$ and $Y(t)$ defined on the same underlying probability space have a *joint CDF* characterized by

$$P_{X(t0)X(t1)\ldots X(tn)Y(t0)\ldots Y(tm)}(x_0, \ldots, x_n, y_0, \ldots, y_m)$$
$$= P(X(t_0) \le x_0, \ldots, X(t_n) \le x_n, Y(t_0) \le y_0, \ldots, Y(t_m) \le y_m) \tag{2.20}$$

for all possible sets of sample times $\{t_0, t_1, \ldots, t_n\}$ and $\{t_0, t_1, \ldots, t_m\}$. Two random processes $X(t)$ and $Y(t)$ are independent if for all such sets we have that

$$P_{X(t0)X(t1)\ldots X(tn)Y(t0)\ldots Y(tm)}(X(t_0) \le x_0, \ldots, X(t_n) \le x_n, Y(t_0) \le y_0, \ldots, Y(t_m) \le y_m)$$
$$= P_{X(t0)X(t1)\ldots X(tn)}(X(t_0) \le x_0, \ldots, X(t_n) \le x_n) P_{Y(t0)\ldots Y(tm)}(Y(t_0) \le y_0, \ldots, Y(t_m) \le y_m) \tag{2.21}$$

➲ The cross-correlation between two random processes $X(t)$ and $Y(t)$ is defined as

$$A_{XY}(t, t+\tau) = \mathbf{E}[X(t)\, Y(t+\tau)]. \tag{2.22}$$

The 2 processes are uncorrelated if $\mathbf{E}[X(t)\, Y(t+\tau)] = \mathbf{E}[X(t)]\, \mathbf{E}[Y(t+\tau)]$ for all t and τ. As with the autocorrelation, if both $X(t)$ and $Y(t)$ are stationary, the cross-correlation is only a function of τ:

$$A_{XY}(t, t+\tau) = \mathbf{E}[X(t-t)\, Y(t+\tau-t)] = \mathbf{E}[X(0)\, Y(\tau)] = A_{XY}(\tau) \tag{2.23}$$

In most analysis of random processes we focus only on the first and second moments.

➲ *Wide-sense stationarity* is a notion of stationarity that only depends on the first two moments of a process, and it can also be easily verified. Specifically, a process is wide-sense stationary (WSS) if it's mean is constant, $\mathbf{E}[X(t)] = \mu_X$, and its autocorrelation depends only on the time difference of the samples,

$$A_X(t, t+\tau) = \mathbf{E}[X(t)\,X(t+\tau)] = A_X(\tau).$$

Stationary processes are WSS but in general WSS processes are not necessarily stationary. For WSS processes, the autocorrelation is a symmetric function of τ , since

$$A_X(\tau) = \mathbf{E}[X(t)X(t+\tau)] = \mathbf{E}[X(t+\tau)X(t)] = A_X(-\tau). \quad (2.24)$$

Moreover, it can be shown that $A_X(\tau)$ takes its maximum value at $\tau = 0$, i.e. $|A_X(\tau)| \leq A_X(0) = \mathbf{E}[X^2(t)]$. As with stationary processes, if two processes $X(t)$ and $Y(t)$ are both WSS then their cross-correlation is independent of time shifts, and thus depends only on the time difference of the processes:

$$A_{XY}(t, t+\tau) = \mathbf{E}[X(0)\,Y(\tau)] = A_{XY}(\tau). \quad (2.25)$$

➲ The *power spectral density* (PSD) of a WSS process is defined as the Fourier transform of its autocorrelation function with respect to τ :

$$Sx(f) = \int_{-\infty}^{+\infty} Ax(\tau)e^{-j2\pi f\tau}\,d\tau \quad (2.26)$$

The autocorrelation can be obtained from a PSD through the inverse transform:

$$Ax(\tau) = \int_{-\infty}^{+\infty} Sx(f)e^{j2\pi f\tau}\,df \quad (2.27)$$

The PSD takes its name from the fact that the expected power of a random process X(t) is the integral of its PSD:

$$E[X^2(T)] = A_X(0) = \int_{-\infty}^{+\infty} Sx(f)df \quad (2.28)$$

The symmetry of $A_X(\tau)$ can be used to show that $S_X(f)$ is also symmetric, i.e. $S_X(f) = S_X(-f)$.

Stationarity and WSS are properties of the underlying probability space associated with a random process. We are also often interested in time-averages associated with random processes, which can be characterized by different notions of *ergodicity*.

➲ A random process $X(t)$ is *ergodic in the mean* if its time-averaged mean, defined as

$$\mu_x^{ta} = \lim_{T\to\infty} \frac{1}{2T} \int_{-T}^{T} Xi(t)dt \quad (2.29)$$

is constant for all possible realizations of $X(t)$. In other words, $X(t)$ is ergodic in the mean if $\lim_{T\to\infty} \frac{1}{2T} \int_{-T}^{T} Xi(t)dt$ equals the same constant μ_x^{ta} for all possible realizations $x_i(t)$ of $X(t)$.

Similarly, a random process $X(t)$ is *ergodic in the nth moment* if its time-averaged *n*th moment

$$\mu_{x^n}^{ta} = \lim_{T\to\infty} \frac{1}{2T} \int_{-T}^{T} X^n(t)dt \quad (2.30)$$

is constant for all possible realizations of $X(t)$. We can also define ergodicity of $X(t)$ relative to its time-averaged autocorrelation

$$A_x^{ta}(\tau) = \lim_{T\to\infty} \frac{1}{2T} \int_{-T}^{T} X(t)X(t+\tau)dt \quad (2.31)$$

➲ $X(t)$ is *ergodic in autocorrelation* if $\lim_{T\to\infty} \frac{1}{2T} \int_{-T}^{T} x_i(t)x_i(t+\tau)dt$ equals the same value $A_x^{ta}(\tau)$ for all possible realizations $x_i(t)$ of $X(t)$. A process that is ergodic in all order moments and autocorrelations is called *ergodic*. Ergodicity of a process requires that its time-averaged *n*th moment and *ij*th autocorrelation, averaged over all time, be constant for all *n*, *i*, and *j*. This implies that the probability associated with an ergodic process is independent of time shifts, and thus the process is stationary. In other words, an ergodic process must be stationary. However, a stationary process can be either ergodic or nonergodic.

2.6 Different types of random processes

Even though there are number of random processes which can be useful to model different systems, a few of them have much importance in wireless applications. These are used to design a reliable communication link between transmitter and receiver depends on the time varying statistical behavior of existing channel. The most useful random processes which are useful to characterize small-scale fading are

- Gaussian random process
- Rayleigh random process
- Ricean random process
- Beta random process
- Gamma process
- Nakagami –m process

2.6.1 Gaussian distribution

A Gaussian random variable is one whose probability density function can be written in the general form

$$f_X(x) = \frac{1}{\sqrt{2\pi\sigma^2}} e^{\frac{-(x-m)^2}{2\sigma^2}} \quad ,-\infty < x < +\infty \tag{2.32}$$

The PDF of the Gaussian random variable has two parameters, m and σ, which have the interpretation of the mean and standard deviation respectively. The parameter σ^2 is referred to as the variance. In general, the Gaussian PDF is centered about the point $x = m$ and has a width that is proportional to σ.

The CDF is required whenever we want to find the probability that a Gaussian random variable lies above or below some threshold or in some interval. The CDF of a Gaussian random variable is written as

$$F_X(x) = \int_{-\infty}^{x} \frac{1}{\sqrt{2\pi\sigma^2}} e^{\frac{-(y-m)^2}{2\sigma^2}} \, dy \tag{2.33}$$

It can be shown that it is impossible to express this integral in closed form.
Because Gaussian random variables are so commonly used in such a wide variety of applications, it is standard practice to introduce a shorthand notation to describe a Gaussian random variable, $X \sim N(m, \sigma^2)$. This is read "X is distributed normally (or Gaussian) with mean, m, and variance, σ^2."

The fallowing figure shows the PDF and CDF of a Gaussian random variable X.

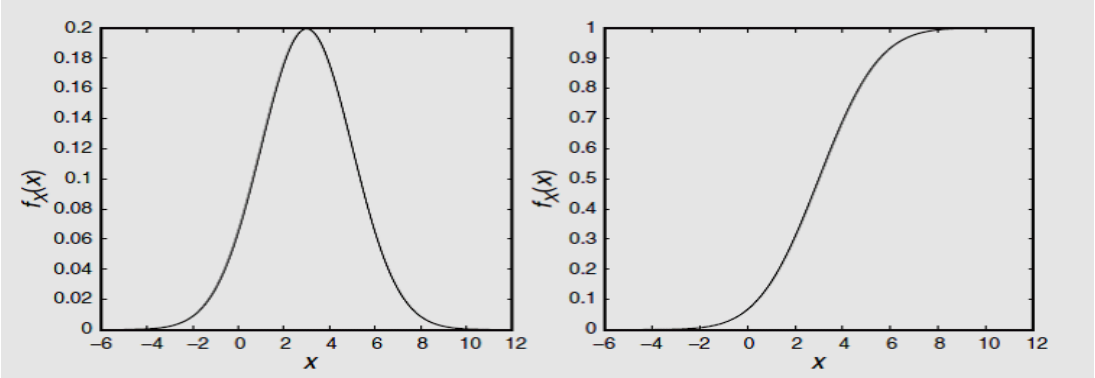

Figure 2.9: PDF and CDF of a Gaussian random variable with $m = 3$ and $\sigma = 2$. [6]

2.6.2 Rayleigh distribution

A Rayleigh random variable has a one-sided PDF. The functional form of the PDF and CDF are given (for any $\sigma > 0$) by

$$f_X(x) = \left(\frac{x}{\sigma^2}\right) exp\left(-\frac{x^2}{2\sigma^2}\right) u(x) \tag{2.34}$$

$$F_X(x) = (1 - exp\left(-\frac{x^2}{2\sigma^2}\right))u(x) \tag{2.35}$$

The fallowing figure shows the PDF and CDF of a Rayleigh random variable X.

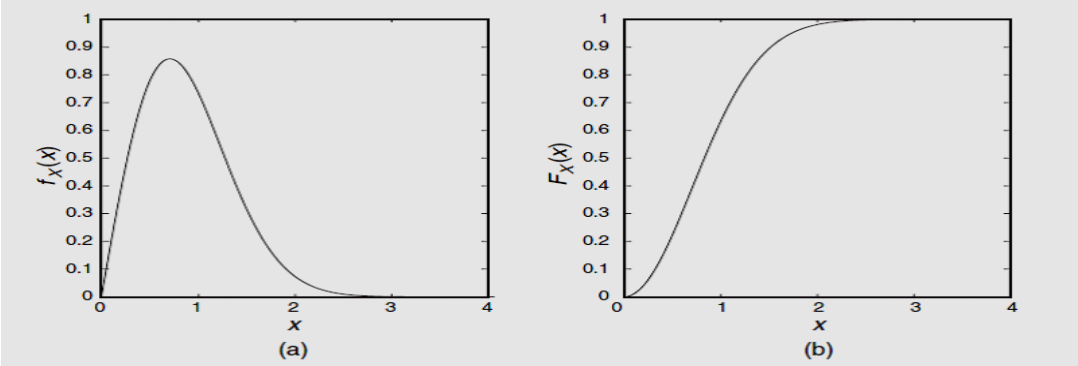

Figure 2.10: PDF and CDF of a Rayleigh random variable, $\sigma^2 = 1/2$. [6]

The Rayleigh distribution is described by a single parameter, σ^2, which is related to the width of the Rayleigh PDF. In this case, the parameter σ^2 is not to be interpreted as the variance of the Rayleigh random variable. The Rayleigh distribution arises when studying the magnitude of a complex number for which real and imaginary parts both follow a zero-mean Gaussian distribution. The Rayleigh distribution arises often in the study of noncoherent communication systems and also in the study of land mobile communication channels, where the phenomenon known as fading is often modeled using Rayleigh random variables.

2.6.3 Ricean distribution

A Rician random variable is closely related to the Rayleigh random variable (in fact, the Rayleigh distribution is a special case of the Rician distribution). The functional form of the PDF for a Rician random variable is given (for any $v > 0$ and any $\sigma > 0$) by

$$f_X(x) = \left(\frac{x}{\sigma^2}\right) exp\left(-\frac{x^2+v^2}{2\sigma^2}\right) I_0\left(\frac{vx}{\sigma^2}\right) u(x) \tag{2.36}$$

In this expression, the function *Io*(*x*) is the modified Bessel function of the first kind of order zero, which is defined by

$$I_0(x) = \frac{1}{2\pi}\int_0^{2\pi} e^{x\cos\theta}\, d\theta \tag{2.37}$$

Like the Gaussian random variable, the CDF of a Rician random variable cannot be written in closed form.

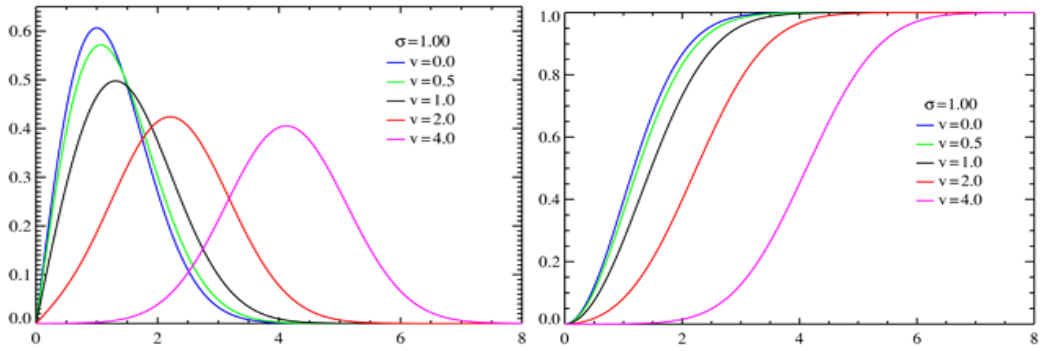

Figure 2.11: PDF and CDF of a Ricean random variable. [12]

2.6.4 Beta distribution

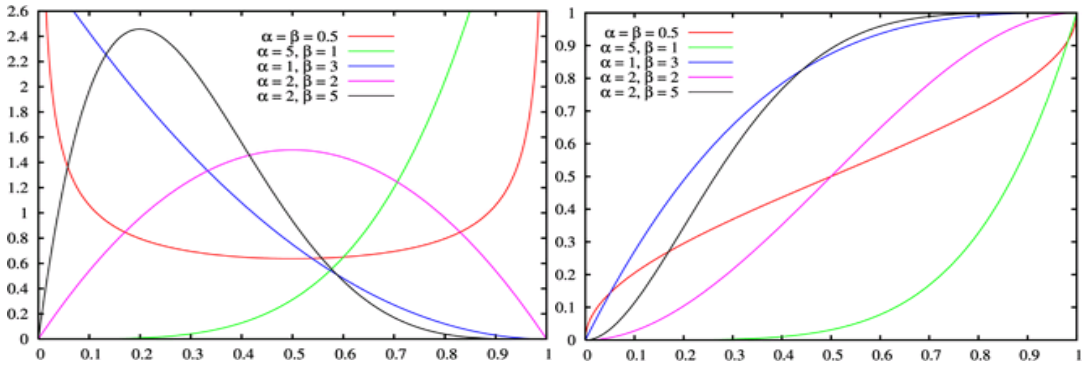

Figure 2.12: PDF and CDF of a Beta distribution [12]

The **beta distribution** is a family of continuous probability distributions defined on the interval [0, 1] parameterized by two positive shape parameters, typically denoted by α and β. The probability density function of the beta distribution is:

$$f_X(x) = \frac{x^{\alpha-1}(1-x)^{\beta-1}}{\int_0^1 u^{\alpha-1}(1-u)^{\beta-1}du}$$

$$= \frac{\Gamma(\alpha+\beta)}{\Gamma(\alpha)\Gamma(\beta)} x^{\alpha-1}(1-x)^{\beta-1}$$

$$= \frac{1}{B(\alpha,\beta)} x^{\alpha-1}(1-x)^{\beta-1} \tag{2.38}$$

where Γ is the gamma function. The beta function, B, appears as a normalization constant to ensure that the total probability integrates to unity. This beta function is defined as

$$B(a,b) = \frac{\Gamma(a)\Gamma(b)}{\Gamma(a+b)} \tag{2.39}$$

2.6.5 Gamma Distribution

The probability density function of the gamma distribution can be expressed in terms of the gamma function parameterized in terms of a shape parameter k and scale parameter θ. Both k and θ will be positive values. The equation defining the PDF and CDF of a gamma-distributed random variable X are given as

$$f_X(x) = \frac{\left({}^{x}/_{\theta}\right)^{k-1} \exp\left({}^{-x}/_{\theta}\right)}{\theta\Gamma(k)} u(x) \quad for\ k, \theta > 0 \tag{2.40}$$

$$F_X(x) = \frac{P\left(k, {}^{x}/_{\theta}\right)}{\Gamma(k)} u(x) \tag{2.41}$$

In the above equations, the gamma function is a generalization of the factorial function defined by

$$\Gamma(\alpha) = \int_0^{\infty} e^{-t} t^{\alpha-1}\, dt \tag{2.42}$$

And the incomplete gamma function is given by

$$P(\alpha, \beta) = \int_0^{\beta} e^{-t} t^{\alpha-1} dt \tag{2.43}$$

The fallowing figure shows the PDF and CDF of Gamma distribution.

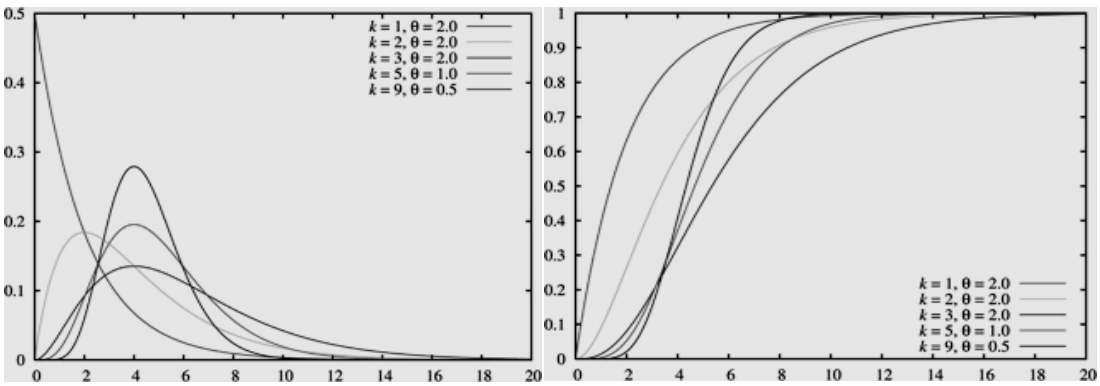

Figure 2.13: PDF and CDF of a Gamma distribution [12]

CHAPTER 3
LITERATURE SURVEY

This chapter gives a brief introduction to Nakagami-m process, its statistical properties and the methods available in literature to generate these random processes.

3.1 Nakagami-*m* distribution

The first work of researching and developing of digital mobile communication system is to understand mobile channel characteristics itself. As we have seen in second chapter, Rayleigh and Rician fading models have been widely used to simulate small scale fading environments over decades. [1] States that Rayleigh fading falls short in describing long-distance fading effects with sufficient accuracy. M. Nakagami observed this fact and then formulated a parametric gamma function to describe his large-scale experiments on rapid fading in high frequency long-distance propagation. Although empirical, the formula is rather elegant and has proven useful.

The **Nakagami distribution** or the **Nakagami-*m* distribution** is a probability distribution related to the gamma distribution. It has two parameters: a shape parameter μ and a second parameter controlling spread, ω. The Nakagami-*m* distribution having the PDF of the form

$$f(x;\mu;w) = \frac{2\mu^{\mu}}{\Gamma(\mu)\omega^{\mu}} x^{2\mu-1} e^{-\frac{\mu}{\omega}x^2} \quad \text{for } x \geq 0 \tag{3.1}$$

Its CDF is given by

$$F(x;\mu;w) = P(\mu, \frac{\mu}{\omega}x^2) \tag{3.2}$$

where *P* is the incomplete gamma function which is defined in (2.43).

The PDF and CDF plots of Nakagami-*m* distribution are shown below.

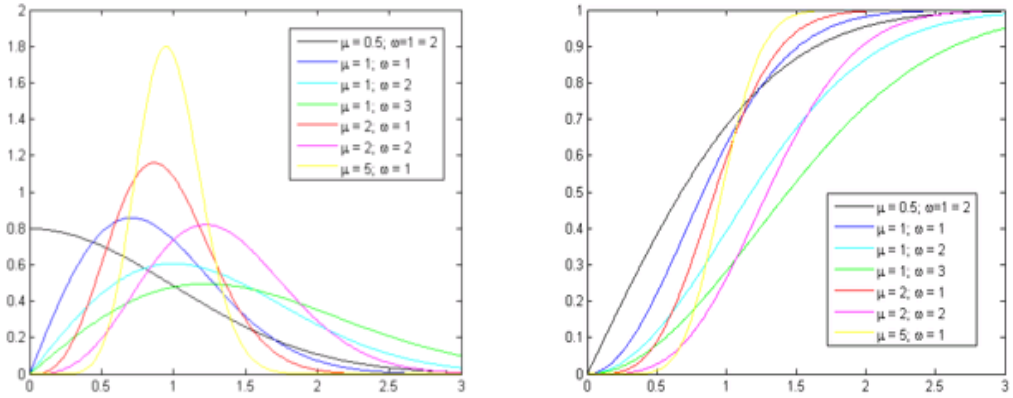

Figure 3.1: PDF and CDF of a Nakagami-*m* distribution [12]

In addition to the m-distribution, the following two compact forms of distributions,

$$p(R) = \frac{2R}{\sigma} e^{\left(-\frac{R^2+{R_0}^2}{\sigma}\right)} I_0\left(\frac{2RR_0}{\sigma}\right) \tag{3.3}$$

$$p(R) = \frac{2R}{\propto\beta} e^{\left\{\left(-\frac{R^2}{2}\right)\left(\frac{1}{\alpha}+\frac{1}{\beta}\right)\right\}} I_0\left(\frac{R^2}{2}\left(\frac{1}{\beta}-\frac{1}{\alpha}\right)\right) \tag{3.4}$$

are presented by Nakagami (1940) and by Nakagami and Sasaki (1942) respectively. The former named "n-distribution" is frequently used in radio engineering and latter, named "q-distribution", also appears in communication problems. More recently, (Nakagami, Wada, Fujimura, 1953) showed that the m-distribution is a more general solution with good approximation to the random vector problem. At the same time it was also shown that m-distribution includes in particular manner the two distributions stated above. Also, the mutual dependencies among their parameters were fully investigated, when m-distribution and the other distributions were fully transformed.

3.1.1 Statistical properties of Nakagami-*m* distribution

The parameters μ and ω are obtained by

$$\mu = \frac{E^2(X^2)}{Var\,[X^2]} \tag{3.5}$$

$$\omega = E[X^2] \tag{3.6}$$

Values of these parameters are μ∈ [0.5 1) and ω >0.

The mean and variance of this distribution are

$$E[X] = \frac{\Gamma\left(\mu+\frac{1}{2}\right)}{\Gamma(\mu)}\left(\frac{\omega}{\mu}\right)^{\frac{1}{2}} \tag{3.7}$$

$$Var(X) = \omega\left(1 - \frac{1}{\mu}\left(\frac{\Gamma(\mu+\frac{1}{2})}{\Gamma(\mu)}\right)^2\right) \tag{3.8}$$

3.1.2 Higher Order Statistics of Nakagami-*m* Distribution

While Nakagami PDF has many attractive features, there is still no widely accepted general and efficient way if simulating a correlated Nakagami fading channel. This is partly due to the fact that no temporal correlation was specified when it was proposed. Therefore most simulators need to make certain assumptions in order to model temporal autocorrelation of a Nakagami fading channel. Some analytical work has been carried out with respect to higher order statistics.

- **Level Crossing Rate (LCR):**

Level Crossing Rate is defined as the number of times per unit duration that the envelope of a fading channel crosses a given value in the negative direction.

- **Average Duration of fades (ADF):**

Average Duration of fades corresponds to the average length of time the envelope remains under the threshold value once it crosses it in the negative direction.

These quantities reflect correlation properties, and thus the second-order statistics, of a fading channel.

Denoting time derivative the envelope r as R' and Level Crossing Rate as R, the LCR occurring at a certain level 'R' is defined as

$$N_R = \int_0^\infty r' p(r', r = R) dr' \tag{3.9}$$

Similarly ADF can be defined as

$$T_R = \frac{prob\,(r \leq R)}{N_R} \tag{3.10}$$

$$T_R = \frac{F_R(r)}{N_R(r)} \tag{3.11}$$

where $F_R(r) = \int_0^r P_R(\propto) d \propto$ is the characteristic function of the channel.

The analysis of LCR and ADF enables one to get the statistics of burst errors occurring on fading channel. This statistics provides useful information for the design of the error-correcting codes, which are complicated by the presence of error bursts. Interleaver size can be optimized based on such statistics. Interleaving is an operation of spreading burst errors into random errors. Further, LCR and ADF have found a variety of applications in the modeling and design of wireless communication systems, such as the finite-state Markov modeling of fading channels, the analysis of hand-off algorithms and the estimation of packet error rates.

[24] Provides the exact formula for LCR and ADF for μ=*n*/2 where n is non-negative integer value. But the simulation has shown that results agree with theoretical results for any m. Analytical LCR and ADF for diversity techniques have been thoroughly considered in [25]. The LCR and ADF expressions are rearranged such that it can be expressed as the product of the PDF of received signal and an integral involving the conditional derivative of this signal. Depending upon different diversity schemes, first term can be found in the literature or can be derived. The conditional PDF in second term can found by examining the expression for derivative of received sign.

3.1.3 Relation to other random variables

I. As mentioned earlier, the Nakagami distribution is related to the gamma distribution. In particular given a random variable Y~ Gamma (k,θ), it is possible to obtain a random variable X~ Nakagami (μ,ω), by setting $k = \mu$, $\theta = \omega / \mu$, and taking the square root of *Y*:

$$X = \sqrt{Y} \tag{3.12}$$

II. When 2μ is an integer, the Nakagami distribution $f_Y(y)$ can be generated from the Chi distribution with parameter k set to 2μ and then following it by the scaling transformation

$$Y = \sqrt{(\omega/2\mu)}X \tag{3.13}$$

Where X is a Chi-squared (χ^2) RV having the PDF of the form

$$f_X(x) = \frac{x^{c-1}\exp\left(-\frac{x}{2}\right)}{2^c\Gamma(c)}u(x), \text{ for } c \geq 0 \quad (3.14)$$

III. From the PDF plot of the Nakagami-*m* distribution, we can easily verify that nakagami-m distribution becomes Rayleigh distribution for *m*=1.

An interesting point to note that is when *m*=0.5, for starting values of X values, the PDF plot is just opposite to that of Rayleigh PDF plot. Of course, it fallows the Rayleigh distribution for next values of X.

IV. Similarly for higher values of nakagami-m distribution i.e., $m \gg 1$, it behaves like the Gaussian distribution.

3.2 Generation of nakagami-m processes

3.2.1 Generation of Nakagami Signals for $m < 1$

In the design of HF communication system, the system designer may want to ensure that the performance of the communication system is satisfactory not only in a Rayleigh fading environment but also in an environment characterized by more severe than Rayleigh fading. The care must be taken while investigating fading phenomenon when $m<1$. This represents more severe fading conditions than Rayleigh fading. To simulate Nakagami fading channels for $m < 1$, one needs to generate complex random process that fits a given Doppler spectrum. Although there are many methods available to simulate Rayleigh fading channels, techniques for simulating an m-fading channel with $m < 1$ are relatively few. According to [1], complex random processes used for simulating an *m*-fading channel, $m< 1$, can be expressed as a product of a complex Gaussian process and a square root beta process. The square root beta process can be realized by a nonlinear transformation of complex Gaussian process. Although this method is efficient, the algorithm developed is too complex to realize. [22] Offers a simple solution to generate fading samples for $m< 1$.

3.2.2 Generation of Uncorrelated Nakagami Signals

The generation of independent Nakagami-*m* random variates is an important problem with many practical applications. For example, the generation of independent Nakagami-*m* random variables is required to simulate the performance of channel estimators [16]-[18] and diverse systems operating in very slow Nakagami-*m* fading channels. Other techniques are use method of rejection to generate samples of Nakagami distribution. Reference [19] gives detailed description and proof of rejection method. This is a simple algorithm to generate uncorrelated Nakagami-*m* samples. The acceptance-rejection method is well known. The challenge in this method is to find the hat function that is both easy to compute and close enough to scaled desired probability density function. The regions $0.5 \leq m < 1$ and $m \geq 1$ represent fundamentally different fading scenarios and should be carefully handled. Suppose we need to generate samples of X with Nakagami-*m* distribution $f_X(x)$. As mentioned above we would look for *hat function* $f_w(X)$, that is easy to generate and which has the property that there exists some constant C, such that

$$C f_w(x) \geq f_X(x) \quad \forall\, x \tag{3.15}$$

Once a suitable $f_w(x)$ has been found, generating samples of Nakagami fading samples is relatively easy. The efficiency of this method is given by 1/C.

Pätzold *et al.* [8] have developed a method for realizing a general fading process by using Rice's sum of sinusoids. However, selection of amplitude values for sinusoids is rather complex except in the special case of $m=1$, that is, if the channel is a Rayleigh fading channel. In this special case, the simulated waveform is a complex Gaussian process and amplitude values are easily determined. Using the proposed model here, for simulating an *m*- fading channel, one can avoid the difficult task of determining amplitude values for sinusoids. Furthermore, the proposed model requires the generation of a complex Gaussian process; simulation using the proposed model can therefore take advantage of the efficient technique developed in [8] for the generation of this process.

In [9], a first-order hidden Markov model is used to model a Nakagami- fading process. This model can be used to generate a fading process that simulates the behavior of the amplitude, say r(t), of an *m*- fading channel. After generating another

random process that simulates the phase, say θ(t), one may generate a complex random process $Z(t) = r(t)e^{j\theta(t)}$ that simulates an *m*-fading channel. The difficulty in the implementation of this approach is to determine autocorrelation functions of r(t) and θ(t) based on a knowledge of the autocorrelation function of z(t), which is usually given in practice.

3.2.3 Generation of Correlated Nakagami Signals

It is well known that Nakagami random variable is a square root of a gamma process and a gamma process itself can be realized from Gaussian random variable. Ertel and Reed [20] designed the method of generating tow correlated Rayleigh fading envelops of equal power. The idea used here is to exploit the fact that the envelope of a complex Gaussian variable follows Rayleigh distribution. The authors therefore were able to correlate the cross-correlation of these Rayleigh envelopes to their counterpart for the corresponding complex Gaussian variables. Until this period, there was no general technique available to simulate Nakagami fading environment. Reference [25] uses a decomposition principle for representing a gamma vector as a direct sum of independent vectors. A set of independent vectors itself can be obtained from a set of correlated Gaussian vectors. The limitation of this method is all branches assume equal fading parameter. This drawback was addressed in reference [21], which offers more realistic model that allows arbitrary fading parameters, branch power and correlation matrix. The author derived a generic characteristic function of correlated Nakagami powered signals allowing all parameters to be arbitrary. [23] Provides a new algorithm to generate Nakagami-m random samples for arbitrary values of m, whereas the author claims that the previous generation methods are restricted to values of m between 0 and 1 and integer and half-integer values of *m*. Finally, [24] proposed a Nakagami-*m* fading simulator by incorporating pop's architecture. They also proposed modified version to generate uncorrelated Nakagami-m fading waveforms through orthogonal Walsh-Hadmard code words. Original Jake's model lacks the property of wide sense stationary. WSS can be achieved by inserting random phase in low frequency oscillators.

Theoretically, the most effective technique to mitigate multi-path fading in a wireless channel is transmitter power control. If channel conditions as experienced by the receiver on one side of the link are known at the transmitter on the other side, the

transmitter can pre distort the signal in order to overcome the effect of the channel at the receiver. There are two fundamental problems with this approach. The major problem is the required transmitter dynamic range. For the transmitter to overcome a certain level of fading, it must increase its power by that same level, which in most cases is not practical because of radiation power limitations and the size and cost of the amplifiers. The second problem is that the transmitter does not have any knowledge of the channel experienced by the receiver except in systems where the uplink (remote to base) and downlink (base to remote) transmissions are carried over the same frequency. Hence, the channel information has to be fed back from the receiver to the transmitter, which results in throughput degradation and considerable added complexity to both the transmitter and the receiver. Moreover, in some applications there may not be a link to feed back the channel information.

3.2.3.1 Antenna diversity:

Diversity is a technique which searches for strongest signal from the multi-path radio signals. The property of technique increases its demand for digital mobile radio services. If one path undergoes very deep fade, other may have strong signal. The diversity process selects the path having strong signal. In most scattering environments, antenna diversity is a practical, effective and, hence, a widely applied technique for reducing the effect of multi-path fading.

There are 2 approaches to reduce the effect of multi path fading.

1. Receive diversity
2. Transmit diversity

- **Receive diversity:**

The classical approach is to use multiple antennas at the receiver and perform combining or selection and switching in order to improve the quality of the received signal. This type of diversity is called receive diversity. The use of multiple antennas and radio frequency (RF) chains (or selection and switching circuits) makes the remote units larger and more expensive but receives diversity increases the SNR by reasonable amount.

- **Transmit diversity:**

There is also another way to implement diversity in which, diversity techniques are applied to base stations to improve their reception quality. This technique is called transmit diversity. A base station often serves hundreds to thousands of remote units. It is therefore more economical but its performance is not as good as receiving diversity.

The explosive growth of wireless systems coupled with the proliferation of laptop and palmtop computers indicate a bright future for wireless networks, both as stand-alone systems and as part of the larger networking infrastructure. However, many technical challenges remain in designing robust wireless networks that deliver the performance necessary to support emerging applications. These challenges transcend all levels of the overall system design including hardware, communication link, network and application design. One of the toughest challenges faced by wireless engineers and system designers is the bottleneck presented by the wireless link layer. Achieving high data rates on the wireless channel is a hard problem for several reasons. The wireless channel is a harsh time-varying propagation environment. A signal transmitted on a wireless channel is subject to:

- Poor BER due to the range, which causes path loss.
- Poor BER due to uniformity of coverage, which causes fading.
- Poor BER due to Frequency reuse which causes co-channel interference.
- Need more capacity (reuse would affect the BER), which causes co-channel interference.

As mentioned above poor BER is the main problem in wireless communication. Let us have a glance on BER. Bit error rate is a parameter which gives an excellent indication of the performance of a data link such as radio or fiber optic system. As one of the main parameters of interest in any data link is the number of errors that occurs so BER is a key parameter.

When data is transmitted over a data link, there is a possibility of errors being introduced into the system. If errors are introduced into the data, then the integrity of the system may be compromised. As a result, it is necessary to assess the performance

of the system, and bit error rate, BER, provides an ideal way in which this can be achieved.

Unlike many other forms of assessment, bit error rate, assesses the full end to end performance of a system including the transmitter, receiver and the medium between the two. In this way, BER enables the actual performance of a system in operation to be tested, rather than testing the component parts and hoping that they will operate satisfactorily when in place.

The main reasons for the degradation of a data channel and the corresponding bit error rate, BER is noise and changes to the propagation path (where radio signal paths are used). Both effects have a random element to them, the noise following a Gaussian probability function while the propagation model follows a Rayleigh model. This means that analysis of the channel characteristics are normally undertaken using statistical analysis techniques.

Diversity can be classifies into following categories:

- Polarization diversity
- Angle diversity
- Frequency diversity
- Time diversity
- Space diversity

Detailed discussion on these different types of diversity is given in [5].

CHAPTER 4

FADING CHANNEL - STATISTICAL MODELS

This chapter explains the different fading models like Rayleigh, Ricean fading channels. A mathematical approach has been given to generate the correlated and uncorrelated Nakagami-m channels.

4.1 Different fading models

The following table shows the different channel characterizations corresponding to the different wireless environments.

ENVIRONMENT	CHANNEL TYPE
Mobile systems with no LOS path between transmitter and receiver antenna, propagation of reflected and refracted paths through troposphere and ionosphere, ship- to- ship radio links.	Rayleigh
Satellite links subject to strong ionospheric scintillation	Nakagami-q (Hoyt) (spans range from one-sided Gaussian (q=0) to Rayleigh (q=1)).
Propagation paths consisting of one strong direct LOC component and many random weaker components- microcellular urban and suburban land mobile, picocellular indoor and factory environments.	Nakagami-*n* (Rice) (spans range from Rayleigh ($n = 0$) to no fading ($n = \bullet$))
Land mobile indoor mobile multipath propagation as well as ionospheric Nakagami-*m* (spans range from one-sided Gaussian radio links.	Nakagami-*m* (spans range from one-sided Gaussian radio links. $m = 1/2$), Rayleigh($m = 1$) to no fading ($m = \bullet$))

Terrain, buildings, trees -urban land mobile systems, land mobile satellite Log-normal shadowing Systems.	Log-normal shadowing
Nakagami-*m* multipath fading superimposed on log-normal shadowing. Composite gamma/log-normal. Congested downtown areas with slow-moving pedestrians and vehicles. Also in land mobile systems subject to vegetative and/or urban shadowing.	Composite gamma/log-normal
Convex combination of unshadowed multipath and a composite multipath/Combined (time-shared) shadowed/unshadowed. Shadowed fading. Land mobile satellite systems.	Combined (time-shared) shadowed/ unshadowed.

Table 4.1: Types of fading models

4.1.1 Rayleigh fading model

In mobile radio channels, the Rayleigh distribution is commonly used to describe the statistical time varying nature of the received envelope of a flat fading signal, or the envelope of an individual multipath component. We consider this model when there is no line-of-sight component between transmitter and receiver. In this, the power is exponentially distributed and phase is uniformly distributed and independent from the amplitude. The fallowing figure shows a Rayleigh distributed signal envelope as a function of time.

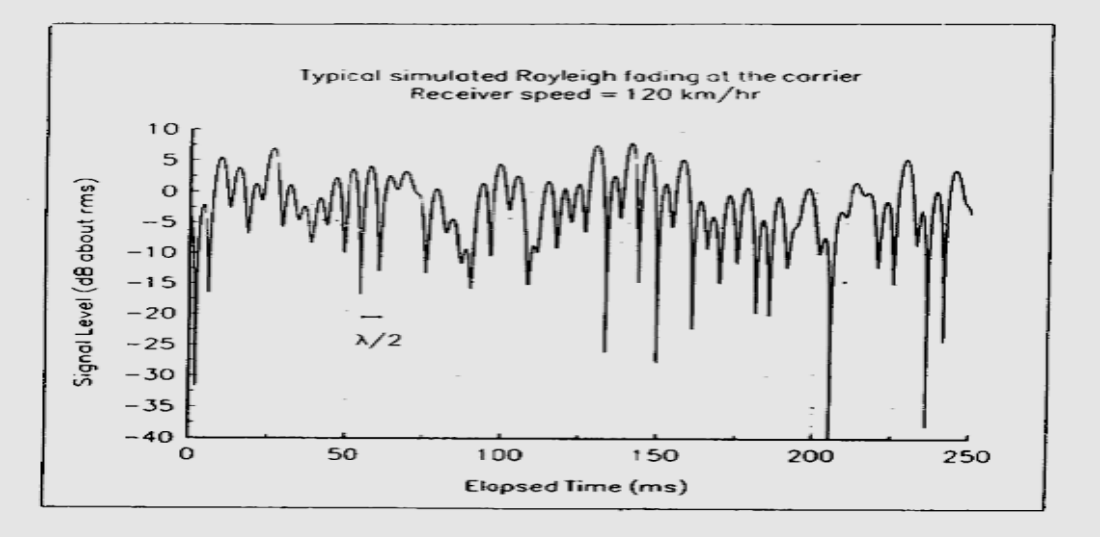

Figure 4.1 A typical Rayleigh fading envelope at 900 MHz [from [Fun93]©IEEE]

The Rayleigh distribution has a PDF given as

$$p(r) = \begin{cases} \frac{r}{\sigma^2} e^{\frac{-r^2}{2\sigma^2}} & (0 \le r \le \infty) \\ 0 & (r < 0) \end{cases} \tag{4.1}$$

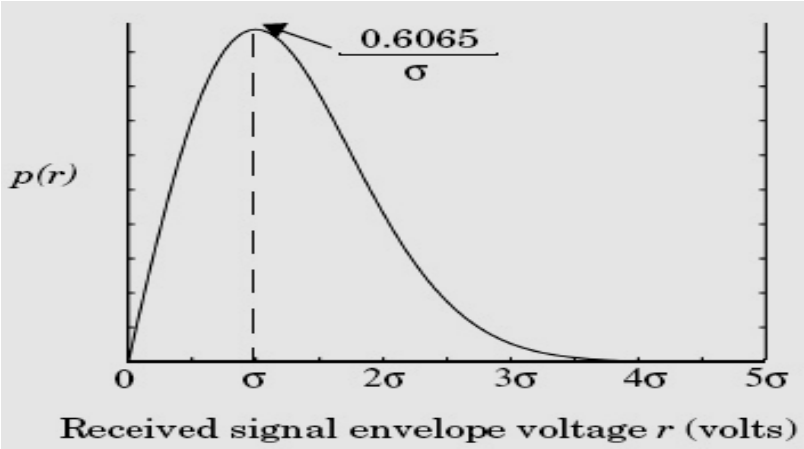

Figure 4.2: Rayleigh PDF [5]

Where σ is the rms value of the received voltage signal before envelope detection, and σ^2 is the time-average power of the received signal before envelope detection. The probability that the envelope of the received signal does not exceed a specified value R is given by the corresponding CDF

$$P(R) = P_r(r \le R) = \int_0^R p(r)dr = 1 - e^{\frac{-r^2}{2\sigma^2}} \tag{4.2}$$

The mean value r_{mean} of the Rayleigh distribution is given by

$$r_{mean} = E[r] = \int_0^R rp(r)dr = \sigma\sqrt{\frac{\pi}{2}} = 1.2533\sigma \quad (4.3)$$

And the variance of the Rayleigh distribution is given byσ_r^2, which represents the ac power in the signal envelope

$$\sigma_r^2 = E[r^2] - E^2[r] = \int_0^R r^2 p(r)dr - \frac{\sigma^2\pi}{2} = 0.4292\sigma^2 \quad (4.4)$$

The rms value of the envelope is the square root of the mean square, or$\sqrt{2}\sigma$, where σ is the SD of the original complex Gaussian signal prior to envelope detection.

The median value of r is found by solving

$$\frac{1}{2} = \int_0^{r_{median}} p(r)dr \quad (4.5)$$

and is given as

$$r_{median} = 1.177\sigma \quad (4.6)$$

Thus, the mean and median differ by only 0.55 dB in a Rayleigh fading signal. By using median values instead of mean values, it is easy to compare different fading distributions.

The fallowing diagram shows the phasor representation of the Rayleigh fading phenomenon.

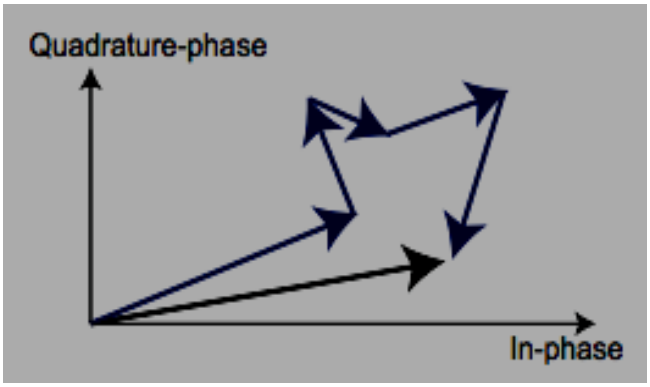

Fig4.3 Phasor diagram of Rayleigh fading envelope

4.1.2 Ricean fading model

When there is a dominant stationary (nonfading) signal component present, such as a line-of-sight propagation path, the small-scale fading envelope distribution is Ricean. In such a situation, random multi path components arriving at different angles are superimposed on a stationary dominant signal. At the output of the envelope detector, this has the effect of adding a dc component to the random multipath.

The fallowing figure shows a Ricean distributed signal envelope as a function of time.

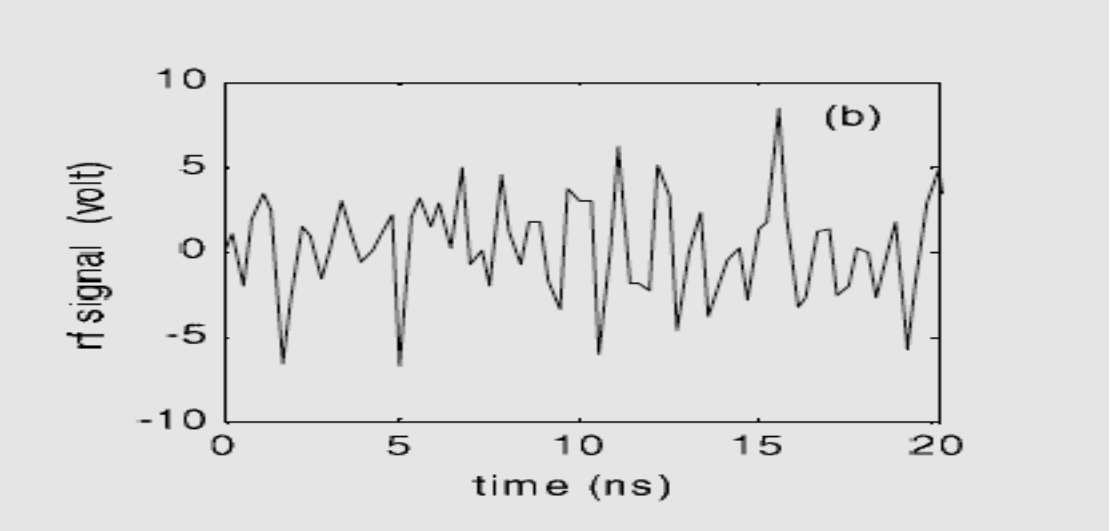

Figure 4.4: A typical Ricean fading envelope at 900 MHz [5]

The PDF of this distribution is given as

$$p(r) = \left(\frac{r}{\sigma^2}\right) exp\left(-\frac{r^2+A^2}{2\sigma^2}\right) I_0\left(\frac{Ar}{\sigma^2}\right) u(r) \tag{4.7}$$

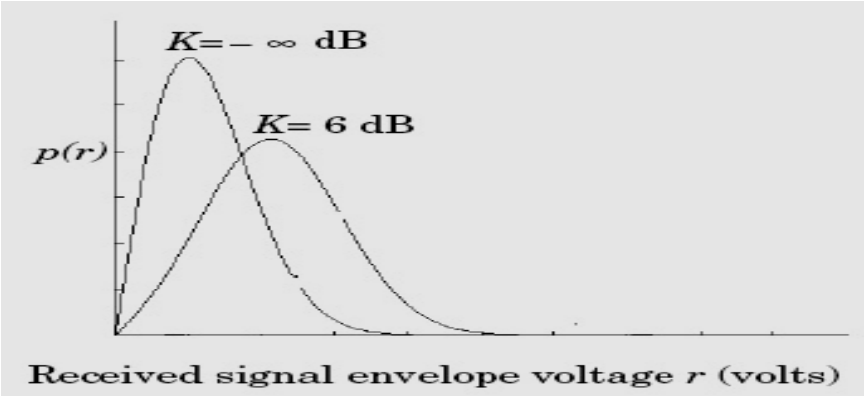

Figure 4.5: PDF of Ricean distributions [5]

The parameter A denotes the peak amplitude of the dominant signal and $I_o(.)$ is the modified Bessel function of the first kind and zero-order. The Rician distribution is often

described in terms of a parameter K which is defined as the ratio between the deterministic signal power and the variance of the multipath. It is given by $K = {A^2}/{2\sigma^2}$

or, in terms of dB

$$K(dB) = 10\log\left({A^2}/{2\sigma^2}\right)dB \tag{4.8}$$

The parameter K is known as the Rician factor and completely specifies the Rician distribution. As $A \to 0, k \to -\infty\ dB$, and as the dominant path decreases in amplitude, the Rician distribution degenerates to a Rayleigh distribution.

The following diagram shows the Phasor representation of Rician fading phenomenon.

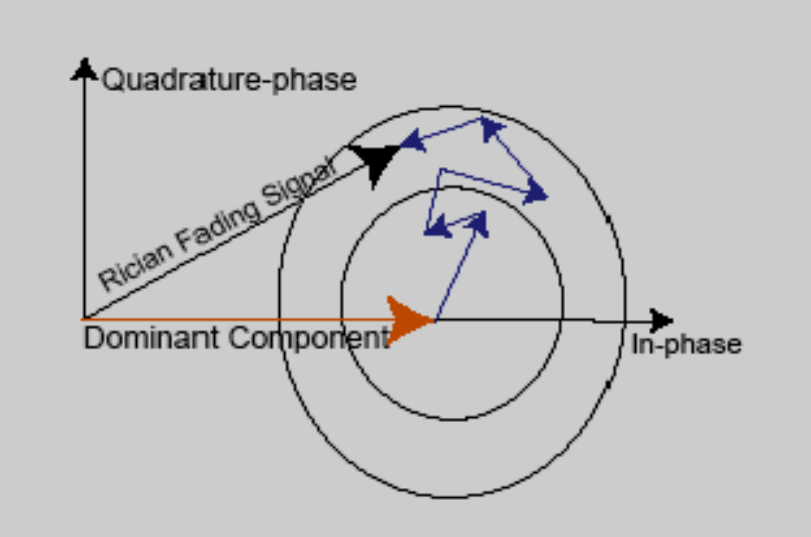

Fig 4.6: Phasor diagram of Rician Fading Envelope

4.2 Nakagami-*m* fading model

It was originally developed based on the empirical results. The phenomenon of fading more severe than Rayleigh fading was observed by Nakagami in a series of channel measurements for some long-distance HF communication links. His measurement results indicate that the *m*- distribution with the fading parameter in the range $0.5 \leq m < 1$ is useful for modeling the fading characteristic of an HF channel when the fading is more severe than Rayleigh fading. Note that the Rayleigh distribution is a special case of the *m*- distribution when *m*=1. It is possible to describe both Rayleigh and Rician fading with the help of a single model using the Nakagami distribution.

The proposed model bypasses generating r(t) and θ(t) separately, so that the difficult task of determining their autocorrelation functions is not required.

To perform computer or hardware simulation of an HF communication link operating over an fading channel for , one is required to generate a complex random process that fits a given Doppler power spectrum where the amplitude follows an distribution with m<1.

Even though there are some existing techniques to simulate the Nakagami-m fading channels as discussed in chapter 3, a better technique is implemented at here which yields the results close to desired ones.

4.3 Problem formulation

4.3.1 Modeling of single channel

Let $Z(t) = r(t)e^{j\theta(t)}$ be a wide-sense stationary (WSS) complex random process that is characterized by the autocorrelation function

$$R_z(\Delta t) = E[z(t)z^*(t+\Delta t)] \tag{4.9}$$

and satisfies the following properties.

1) r (t) is Nakagami-m Distributed with the second moment $\Omega=R_z(0)$ and the fading parameter $m= \Omega^2/E[(r(t)^2- \Omega)^2]$ limited in the range $m \in [0.5, 1)$.
2) θ (t) is uniformly distributed over [0, 2π).
3) r (t) and θ(t) are mutually independent.

The PDF of r (t) for an arbitrary time is given by [2]

$$p(r(t)=r) = \frac{2}{\Gamma(m)}\left(\frac{m}{\Omega}\right)^m r^{2m-1}e^{\frac{-mr^2}{\Omega}}, r \geq 0 \tag{4.10}$$

where Γ(.) is the gamma function and m is in the range $0.5 \leq m < 1$. Our task is to develop a simulation model that can be used to realize z (t). In the development of this model, the following lemma is considered.

Lemma 1: Let be r_z being an m distributed random variable with the second moment $E[r_z^2] = \Omega$ and the fading parameter $m \in [0.5, 1)$. Let r_w be a Rayleigh distributed random variable with $E[r_w^2] = \Omega/m$. If r_z and r_w satisfy the functional relationship

$$r_z = \sqrt{\xi} r_w \tag{4.11}$$

where ξ is a nonnegative random variable independent of r_w, then ξ has a standard beta distribution with parameters *m* and 1-*m*. The PDF of is given by [12]

$$p(\xi) = \begin{cases} \frac{1}{B(m,1-m)} \xi^{m-1}(1-\xi)^{(1-m)-1}, & 0 < \xi < 1 \\ 0 & otherwise \end{cases} \quad (4.12)$$

where $B(a,b) = \Gamma(a)\Gamma(b) \Big/ \Gamma(a+b)$ is a beta function.

Let θ be a random variable uniformly distributed over [0, 2π) and independent of r_z, r_w and ξ. It follows that $w = r_w e^{j\theta}$ is a zero-mean complex Gaussian random variable with uncorrelated real and imaginary parts. Multiplying both sides of (4.11) $e^{j\theta}$ by gives

$$r_z e^{j\theta} = \xi^{1/2} w. \quad (4.13)$$

This expression implies that z (t) can be represented by

$$Z(t) = \mu(t) w(t) \quad (4.14)$$

where

i) $\mu(t)$ is a WSS nonnegative random process and $\mu^2(t)$follows a standard beta distribution with parameters *m* and 1-*m*, and

ii) w(t), being independent of $\mu(t)$, is a zero-mean WSS complex Gaussian process with uncorrelated real and imaginary parts and with an autocorrelation function $R_w(\Delta t) = E[w(t)w^*(t+\Delta t)]$ satisfying $R_w(0) = \Omega/m$.

Notice that $R_w(\Delta t)$ and $R_z(\Delta t)$ are related by

$$R_z(\Delta t) = R_\mu(\Delta t) R_w(\Delta t) \quad (4.15)$$

where $R_\mu(\Delta t) = E[\mu(t)\mu(t+\Delta t)]$ and that $R_\mu(0) = m$.

The representation of Z (t) given by (4.14) is the desired simulation model. One can generate *Z (t) by* generating a complex Gaussian process *w (t)* and an appropriate square-root-beta random process *μ (t)*, followed by substituting *w (t)* and *μ (t)* into (4.14). The non-Gaussian process *μ (t)* which is called as square root bet process can be generated by a nonlinear transformation of a Gaussian process as discussed in section 4.3.3. The complex Gaussian process *w (t)* can be generated by an established technique as discussed in section 4.3.4.

4.3.2 Modeling of correlated diversity channels

Antenna diversity is a well-known technique in HF communications for combating adverse effects due to fading. So far our discussion has been concentrated on simulating an *m* fading channel by generating a complex random process z(t). This approach is useful for simulating a communication system with antenna diversity only if the diversity branches are independently faded. When the antenna spacing is inadequate, nonindependent fading among diversity branches occurs so that the *m* fading channels used for modeling the diversity channels are correlated. It gives rise to the need for simulating correlated diversity channels. In what follows, a method is demonstrated to simulate correlated *m* fading channels for $m<1$ by a simple extension of the model explained in section 4.3.1.

Let *M* be the order of diversity. We assume that the diversity channels have the same fading parameter *m*, second moment Ω, and autocorrelation function $R_z(\Delta t)$. This assumption is appropriate for a communication system using antenna diversity. In the implementation of simulation, one is given knowledge of the correlation matrix $\rho = [\rho_{k,l}]_{k,l=1}^{M}$ that characterizes the correlation among the *M* diversity channels, where $|\rho_{k,l}| \leq 1, \rho_{k,l} = 1$ and ρ is real symmetric. To simulate *M* correlated channels, it is required to generate *M* correlated complex processes $z_k(t)$, k=1, 2…*M*, each of which has the properties of specified in Section 4.3.1. Note that

$$\rho_{k,l} = \frac{E[z_k(t)z_l^*(t)]}{\sqrt{E[|z_k(t)|^2]E[|z_l(t)|^2]}} \tag{4.16}$$

and that ρ is nonnegative definite ([14], p. 295). Applying the proposed model (4.14) to the situation under consideration, we have

$$z_k(t) = \mu_k(t)w_k(t), \qquad k = 1, \dots, M$$

where

i) $\mu_k(t)$ is a WSS nonnegative random process and $\mu_k{}^2(t)$ has a standard beta distribution with parameters *m* and 1-*m*

ii) $w_k(t)$, being independent of $\mu_k(t)$, is a zero-mean WSS complex Gaussian process with uncorrelated real and imaginary parts and with a variance given by Ω/*m*.

We assume that i) any pair of $\mu_k(t)$and $w_l(t), \mathrm{k}, \mathrm{l} = 1, \dots, \mathrm{M}$ are independent, and ii) $\mu_k(t)$and $\mu_l(t), \mathrm{k} \neq \mathrm{l}$ are mutually independent. Assumption i) is made because it

makes implementation easier and does not affect resultant statistical properties of $z_k(t)$'s. Assumption ii) leads to conditions that are usually satisfied in practice. Substituting $z_k(t)$ into (4.16) yields

$$\rho_{k,l} = \begin{cases} K_m \rho_{k,l}^{(w)} & k \neq l \\ \rho_{k,l}^{(w)} & k = l \end{cases} \tag{4.17}$$

where

$$\rho_{k,l}^{(w)} = \frac{E[w_k(t) w_l^*(t)]}{\sqrt{E[|w_k(t)|^2] E[|w_l(t)|^2]}} \tag{4.18}$$

and

$$K_m = \frac{E[\mu_k(t)] \times E[\mu_l(t)]}{\sqrt{E[{\mu_k}^2(t)] E[{\mu_l}^2(t)]}} = \frac{4}{\pi m} \left[\frac{\Gamma(m+0.5)}{\Gamma(m)}\right]^2 \tag{4.19}$$

With knowledge of $\rho_{k,l}$, one can determine $\rho_{k,l}^{(w)}$ by (4.17). Since Autocorrelation functions of $z_k(t)$ are assumed the same for all k's and are given by $R_z(\Delta t)$, for convenience in the implementation, we assume that autocorrelation functions of $\mu_k(t)$'s and $w_k(t)$'s are given by $R_\mu(\Delta t)$ and $R_w(\Delta t)$, respectively, both of which are independent of k. Note that $R_z(\Delta t), R_\mu(\Delta t)$, and $R_w(\Delta t)$ are related by (4.15). After$R_\mu(\Delta t)$ is determined, one can generate each of $\mu_k(t), k = 1, \dots, M$, by a nonlinear transformation of a Gaussian process dictated in section (4.3.3).

Generation of **w** (t) = $[w_1(t), \dots, w_m(t)]^T$ can be accomplished by the following method. Let $u_k(t), k = 1, \dots, M$, be mutually independent zero-mean complex Gaussian processes, each of which has an autocorrelation function $R_w(\Delta t)$ and uncorrelated real and imaginary parts. Each of $u_k(t)$'s can be generated by a known method. Let **u** (t) = $[u_1(t), \dots, u_m(t)]^T$ and $\rho^{(w)} = [\rho_{k,l}^{(w)}]_{k,l=1}^M$. Then

$$\boldsymbol{w}(t) = \mathbf{C}\boldsymbol{u}(t). \tag{4.20}$$

where **C** is a factor of $\rho^{(w)}$ such that $\mathrm{C}\mathrm{C}^T = \rho^{(w)}$.

To generate **w** (t), the matrix **C** must exist, which requires that$\rho^{(w)}$ is nonnegative definite. That is, for any $a_1, a_2, \dots, a_M$ with at least one of which is nonzero, the condition $\sum_{k=1}^M \sum_{l=1}^M a_k a_l \rho_{k,l}^{(w)} \geq 0$ needs to be satisfied. Substituting (4.17) into this requirement yields

$$\sum_{k=1}^M \sum_{l=1}^M a_k a_l \, \rho_{k,l} - (1 - K_m) \sum_{k=1}^M a_k^2 \geq 0 \tag{4.21}$$

It is known that (4.21) can be satisfied if 1-K_m is less than the smallest Eigen value of ρ. As a practical example, consider a dual-diversity system (M=2). The smallest Eigen value is $1 - \rho_{1,2}$, so that (4.21) is satisfied if $\rho_{1,2} \leq K_m$. It can be shown that the

minimum value of K_m over the range $0.5 \leq m < 1$ is 0.8106. As the correlation between diversity channels seldom exceeds 0.8106 for practical cases of interest, (4.21) is usually satisfied. For diversity channels with 1-K_m greater than the smallest Eigen value of ρ, $z_k(t)$'s can be generated by allowing $\mu_k(t)$'s to be correlated.

4.3.3. Generation of square root beta process

The square root beta process $\mu(t)$ can be generated by the nonlinear transformation of the Gaussian Random process given as [13]

$$\mu(t) = F^{-1}\left(\phi\big(y(t)\big)\right) \tag{4.22}$$

where *y(t)* is a zero-mean unit-variance Gaussian process with an autocorrelation function

$$\rho(\Delta t) = E[y(t)y(t+\Delta t)]. \tag{4.23}$$

Let *F(x)* be the CDF of a squire root beta random variable with parameters *m* and 1-*m*, and let $\phi(x)$ be the CDF of a standard Normal random variable. It fallows that

$$F(x) = I_{x^2}(m, 1-m), \quad 0 \leq x \leq 1 \tag{4.24}$$

and

$$\emptyset(\boldsymbol{x}) = \frac{1}{\sqrt{2\pi}} \int_{-\infty}^{\mathrm{x}} \mathrm{e}^{\frac{-\mathrm{t}^2}{2}}\, \mathrm{dt} \tag{4.25}$$

respectively, where $I_u(a,b) = \big(B(a,b)\big)^{-1} \int_0^u t^{a-1}(1-t)^{b-1}dt$ is the incomplete beta function. Note that in the special case of *m*=0.5,

$$F(x) = \frac{2}{\pi}\sin^{-1} x \quad \text{for } 0 \leq x \leq 1. \tag{4.26}$$

It is easy to show that *F(x)* is strictly increasing function for $0 \leq x \leq 1$ and is bounded by $F(x) \in [0,1]$. If we specify that $F^{-1}(v)$, the inverse of *F*, gives a value within [0, 1] for $0 \leq v \leq 1$, then F^{-1} exists and is unique. Let *y(t)* be a WSS zero-mean unit-variance Gaussian random process with an autocorrelation function $\rho(\Delta t) = E[y(t)y(t+\Delta t)]$.

It is known that $\mu(t)$ can be generated by the nonlinear transformation [13,Ch. 3.1.1]

$$\mu(t) = g(y(t)) \tag{4.27}$$

where $g(x) = F^{-1}(\emptyset(x))$. In addition,$R_\mu(\Delta t)$ and $\rho(\Delta t)$ are related by [13, eq. (3.7)]

$$R_{\mu}(\Delta t) = \int_{-\infty}^{\infty}\int_{-\infty}^{\infty} g(y_1)g(y_2)\frac{1}{2\pi\sqrt{1-\rho(\Delta t)^2}}.e^{\left[-\frac{y_1^2+y_2^2-2\rho(\Delta t)y_1y_2}{2(1-\rho(\Delta t)^2)}\right]}dy_1dy_2, \rho(\Delta t) = \pm 1 \quad (4.28)$$

In special cases of $\rho(\Delta t) = \pm 1$, it is easy to show that

$$R_{\mu}(\Delta t) = \begin{cases} m, & \rho(\Delta t) = +1 \\ \int_0^1 F^{-1}(x)\,F^{-1}(1-x)dx, & \rho(\Delta t) = +1. \end{cases} \quad (4.29)$$

4.3.4 Generation of WSS complex Gaussian Process

A zero-mean complex WSS Gaussian process $\mu(t)$ can be realized with the established technique [8] known as rice's sum of sinusoids as explained below.

To find an analytical model which generates a complex Gaussian Process, firstly we should to consider the shape of the Doppler PSD under observation. For mobile fading channel models, a typical and often-assumed shape for the Doppler PSD of the complex Gaussian noise process $\mu(t)$, $S_{\mu\mu}(f)$, is given by the Jakes PSD

$$S_{\mu\mu}(f) = \begin{cases} \frac{2\sigma_0^2}{\pi f_{max}\sqrt{1-\left[\frac{f}{f_{max}}\right]^2}}, & |f| \le f_{max} \\ 0, & |f| > f_{max} \end{cases} \quad (4.30)$$

where f_{max} is the maximum Doppler frequency. From this equation, the corresponding ACF, i.e., the inverse Fourier transform of$S_{\mu\mu}(f)$, is given the following relation:

$$r_{\mu\mu}(t) = 2\sigma_0^2 J_0(2\pi f_{max}\,t) \quad (4.31)$$

where $J_0(.)$ denotes the zeroth-order Bessel function of the first kind.

The resulting structure of the analytical model for complex GRP is shown in the fallowing figure.

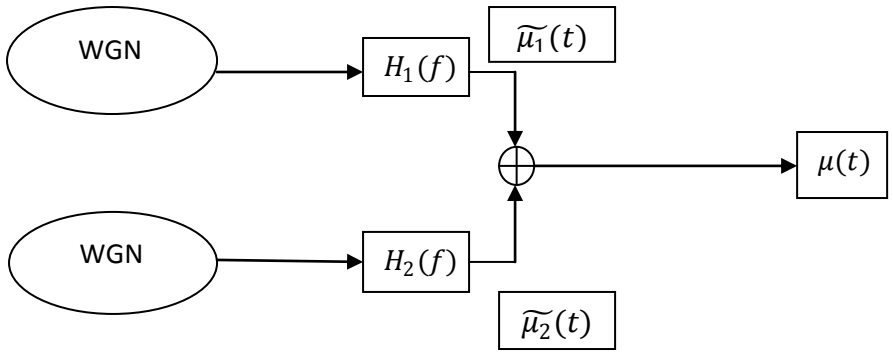

Figure 4.7: Analytical models for generation of complex Gaussian process $\mu(t)$

Instead of generating $\widetilde{\mu_i}(t)$ with the process of passing of a white Gaussian noise (WGN) process through a band pass filter having transfer function $H_i(f)$, it can be generating from a specified number of sinusoids as explained below.

Let us proceed by considering the two real zero mean, equal variance functions $\widetilde{\mu_1}(t)$ and $\widetilde{\mu_2}(t)$, which will be expressed as follows:

$$\widetilde{\mu_i}(t) = \sum_{n=1}^{N_i} c_{i,n} \cos\left(2\pi f_{i,n} t + \theta_{i,n}\right), \qquad i = 1,2 \tag{4.32}$$

where N_i denotes the number of sinusoids of the function $\widetilde{\mu_i}(t)$. The quantities $c_{i,n}, f_{i,n}$ and $\theta_{i,n}$ are simulation model parameters, which are adapted to the desired Doppler PSD function and are therefore called Doppler coefficients, discrete Doppler frequencies, and Doppler phases, respectively. It is worth mentioning that the simulation model parameters $c_{i,n}, f_{i,n}$ and $\theta_{i,n}$ have to be computed during the simulation setup phase, e.g., by any one of the fallowing methods.

- Method of equal distances
- Mean square-error method
- Jakes method
- Optimal solution for the given number of sinusoids

The parameters are calculated at here according to the optimal solution for the given number of sinusoids.

Afterwards, these parameters are known quantities and are kept constant during the whole simulation run phase. From the fact that all parameters are known quantities, it follows that itself is determined for all time and thus can be considered as a deterministic function. We will see that the statistical properties of $\widetilde{\mu_i}(t)$ approximate closely the statistical properties of colored Gaussian stochastic processes. In order to emphasize that property, we will denote henceforth the deterministic function as a *deterministic (Gaussian) process*. Consequently, the interpretation of $\widetilde{\mu_i}(t)$ as a deterministic process (function) allows us to compute an analytical expression for the corresponding ACF via the definition

$$\tilde{r}_{\mu_i\mu_i}(t) = \lim_{T\to\infty} \frac{1}{2T_0} \int_{-T_0}^{T_0} \widetilde{\mu_i}(\tau)\widetilde{\mu_i}(t+\tau)d\tau \tag{4.33}$$

Substituting (4.32) into (4.33) and taking thereupon the Fourier transform, we find the following analytical expressions for the ACF $\tilde{r}_{\mu_i\mu_i}(t)$ and the corresponding PSD $\tilde{S}_{\mu_i\mu_i}(f)$:

$$\tilde{r}_{\mu_i\mu_i}(t) = \sum_{n=1}^{N_i} \frac{{c_{i,n}}^2}{2} \cos\left(2\pi f_{i,n} t\right) \tag{4.34}$$

$$\tilde{S}_{\mu_i\mu_i}(f) = \sum_{n=1}^{N_i} \frac{{c_{i,n}}^2}{4} [\delta\left(f - f_{i,n}\right) + \delta\left(f + f_{i,n}\right)] \text{ for } i = 1,2 \tag{4.35}$$

Notice that the deterministic processes $\widetilde{\mu_1}(t)$ and $\widetilde{\mu_2}(t)$ are uncorrelated if and only if $f_{1,n} \neq \pm f_{2,n}$ for all $n = 1,2,\dots,N_1$ and $m = 1,2,\dots,N_2$. But if $f_{1,n} \neq \pm f_{2,n}$ is valid for some or all *n*, m, then $\widetilde{\mu_1}(t)$ and $\widetilde{\mu_2}(t)$ are correlated, and the following cross-correlation function can be derived, where $N = \min(N_1, N_2)$.

$$\tilde{r}_{\mu_1\mu_2}(t) = \begin{cases} \sum_{n=1}^{N} \frac{c_{1,n}c_{2,m}}{2} \cos\left(2\pi f_{1,n} t - \theta_{1,n} \pm \theta_{2,m}\right) & if \ f_{1,n} = \pm f_{2,m} \\ 0, & if \ f_{1,n} \neq \pm f_{2,n} \end{cases} \tag{4.36}$$

The next figure shows the resulting general structure of the deterministic simulation model for complex Gaussian random process in its continuous-time representation.

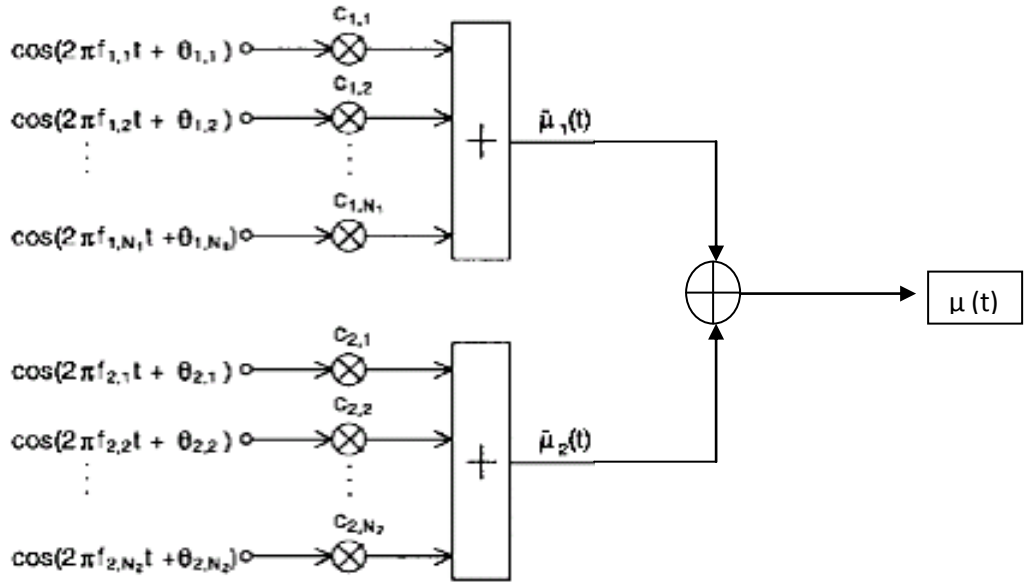

Figure 4.8: Deterministic simulation models for complex GRP with given jakes PSD

As said before, the parameters $C_{i,n}$ and $f_{i,n}$ can be calculated at here according to the optimal solution[8] for the given number of sinusoids. Optimal solution means in the fallowing 2 senses.

1) The PDF of the deterministic process is according to the L_2 norm, an optimal approximation of the ideal (desired) PDF of the stochastic process $\mu_i(t)$.
2) The ACF of the deterministic process is according to L_2 norm, an optimal approximation of the ideal (desired) ACF of the stochastic process $\mu_i(t)$ within a distinct time interval.

The resulting parameters can be calculated from the following formulas. [8]

$$C_{i,n} = \sigma 0\sqrt{(2/N_i)} \qquad \text{for } N_i \geq 7 \tag{4.37}$$

$$f_{i,n} = f_{max} \sin(\pi n/2N_i) \quad \text{for all } n=1,2,\ldots N_i \text{ and } i=1,2. \tag{4.38}$$

CHAPTER5

SIMULATION AND RESULTS

In this chapter, the simulation steps to perform simulation of Nakagami-m channel using the mathematical tool MATLAB R2007b (7.5) has been given. Simulation results are analyzed and compared with the desired values.

5.1 Simulation Steps

For the given PSD $S_z(f)$, it is desired to realize a complex random process z(t) in order to simulate a Nakagami-*m* fading channel for *m*<1. We know that ACF and PSD are Fourier transform pair related as follows:

$$S_z(f) = \int_{-\infty}^{\infty} e^{-j\,2\pi f\,\Delta t}\, R_z(\Delta t) d\Delta t \qquad (5.1)$$

The PSD of the most of the practical HF channels are band-limited, so it is sufficient to generate a band limited random process Z (t).

Let f_{max} be the frequency such that $S_z(f) = 0$ or negligible for $|f| > f_{max}$. To realize samples $Z(nT_s)$, $T_s = {}^{1}/_{\alpha f_{max}}$, and $n = 0, \pm 1, \pm 2, \ldots$. where α is the oversampling factor and $\alpha \geq 8$ is usually sufficient to generate Z (t) without appreciable loss of accuracy. The remaining simulation steps to generate required process are given as fallows.

Step 1:

Compute $R_z(\Delta n t_s), \Delta n = -N, \ldots, N$, where N is sufficiently large integer. This sequence of $R_z(\Delta n t_s)$ is used in generating $Z(nT_s)'$s so that greater value of N improves the accuracy of the ACF of the generated $Z(nT_s)'$s.

Step 2:

Select an appropriate $\rho(\Delta t)$. From the equation, it is clear that $S_z(f)$ is given by the convolution between the PSDs of $\mu(t)$ and $w(t)$, and since Z(t) is band-limited to f_{max} , so that $\mu(t)$ and $w(t)$ are also band-limited to at most f_{max}. As $\mu(t)$ is generated from *y (t* , it is also band-limited to at most f_{max} . Now, choose $\rho(\Delta t)$ such that

$$S_y(f) = \int_{-\infty}^{\infty} e^{-j2\pi f \Delta t}\, \rho(\Delta t) d\Delta t \tag{5.2}$$

vanishes or negligible for $|f| > f_{max}$.

Step 3:

Compute $R_\mu(\Delta n t_s)$ from $\rho(\Delta n T_s)$ with the help of table 5.1. Then compute $R_w(\Delta n t_s)$'s as

$$R_w(\Delta n T_s) = \frac{R_z(\Delta n T_s)}{R_\mu(\Delta n T_s)} \tag{5.3}$$

To ensure that w (t) can be realized, $R_w(\Delta t)$ is required to satisfy that $|R_w(\Delta t)| \leq R_w(0)$ and $S_w(f) \geq 0$ for all f, where $R_w(\Delta t)$ and $S_w(f)$ are Fourier transform pair.

If the selected $\rho(\Delta t)$ cannot yield $R_w(\Delta n T_s)$'s that satisfy $|R_w(\Delta t)| \leq R_w(0)$, another choice of $\rho(\Delta t)$ should be made, and step (2) should be repeated. From this $R_w(\Delta n T_s)$, $S_w(f)$ can be calculated as

$$S_w(f) = \begin{cases} T_s\{R_w(0) + 2\sum_{\Delta n=1}^{N} \mathrm{Re}[R_w(\Delta n T_s).e^{-j2\pi f \Delta n T_s}]\}, & |f| \leq {}^{1}/_{2T_s} \\ 0, & other\ wise. \end{cases} \tag{5.4}$$

If this computed $S_w(f)$ is negative and not limited to f_{max} , then it has to modify such that

$$S_w(f) \geq 0 \;\&\; S_w(f) = 0 \;\forall\; f > f_{max} .$$

This modified $S_w(f)$ can be used to compute new values of $R_w(\Delta n T_s)$.

Step 4:

With the selected $\rho(\Delta t)$ or $S_y(f)$, $y(nT_s)$ can be generated by the method specified in the section4.3.4. Next, square root beta process samples $\mu(nT_s)$ can be generated from $y(nT_s)$ by the method specified in the section 4.3.2.

Step 5:

Generate complex Gaussian distributed samples $w(nT_s)$ based on the modified $S_w(f)$ or the new values of $R_w(\Delta n T_s)$ with the help of the method specified in the section 4.3.4.

Step 6:

Compute $z(nT_s)$ as

$$Z(nT_s) = w(nT_s)\mu(nT_s) \tag{5.5}$$

$\rho(\Delta t)$	$R_\mu(\Delta t)/R_\mu(0)$									
	$m = 0.5$	0.55	0.6	0.65	0.7	0.75	0.8	0.85	0.9	0.95
−1.0	0.6366	0.7028	0.7612	0.8122	0.8562	0.8936	0.9248	0.9503	0.9708	0.9871
−0.9	0.6550	0.7162	0.7704	0.8180	0.8594	0.8951	0.9253	0.9504	0.9708	0.9871
−0.8	0.6728	0.7297	0.7801	0.8245	0.8634	0.8972	0.9262	0.9507	0.9709	0.9871
−0.7	0.6906	0.7433	0.7901	0.8314	0.8679	0.8998	0.9275	0.9511	0.9710	0.9871
−0.6	0.7096	0.7569	0.8003	0.8388	0.8728	0.9028	0.9291	0.9518	0.9711	0.9871
−0.5	0.7252	0.7706	0.8108	0.8465	0.8782	0.9063	0.9311	0.9527	0.9714	0.9872
−0.4	0.7424	0.7843	0.8215	0.8545	0.8840	0.9101	0.9334	0.9539	0.9719	0.9872
−0.3	0.7594	0.7980	0.8323	0.8628	0.8900	0.9143	0.9360	0.9553	0.9725	0.9874
−0.2	0.7764	0.8119	0.8434	0.8714	0.8964	0.9188	0.9390	0.9570	0.9732	0.9875
−0.1	0.7934	0.8259	0.8546	0.8802	0.9031	0.9237	0.9422	0.9590	0.9741	0.9878
0.0	0.8106	0.8400	0.8660	0.8893	0.9101	0.9288	0.9458	0.9612	0.9753	0.9881
0.1	0.8278	0.8543	0.8777	0.8986	0.9173	0.9342	0.9496	0.9636	0.9766	0.9886
0.2	0.8452	0.8688	0.8896	0.9082	0.9249	0.9400	0.9537	0.9663	0.9781	0.9891
0.3	0.8628	0.8835	0.9018	0.9181	0.9328	0.9460	0.9581	0.9693	0.9798	0.9898
0.4	0.8808	0.8986	0.9143	0.9284	0.9410	0.9524	0.9629	0.9726	0.9818	0.9907
0.5	0.8990	0.9140	0.9272	0.9390	0.9496	0.9592	0.9680	0.9762	0.9840	0.9916
0.6	0.9178	0.9299	0.9405	0.9500	0.9586	0.9663	0.9734	0.9801	0.9865	0.9928
0.7	0.9370	0.9463	0.9544	0.9615	0.9680	0.9739	0.9793	0.9843	0.9892	0.9942
0.8	0.9570	0.9633	0.9688	0.9736	0.9780	0.9819	0.9856	0.9890	0.9924	0.9958
0.9	0.9780	0.9812	0.9839	0.9864	0.9886	0.9906	0.9924	0.9942	0.9959	0.9977
1.0	1.0000	1.0000	1.0000	1.0000	1.0000	1.0000	1.0000	1.0000	1.0000	1.0000

Table 5.1: $R_\mu(\Delta t)/R_\mu(0)$ values against $\rho(\Delta t)$ for $0.5 \leq m < 1$. [1]

The flowchart of this simulation method is given below.

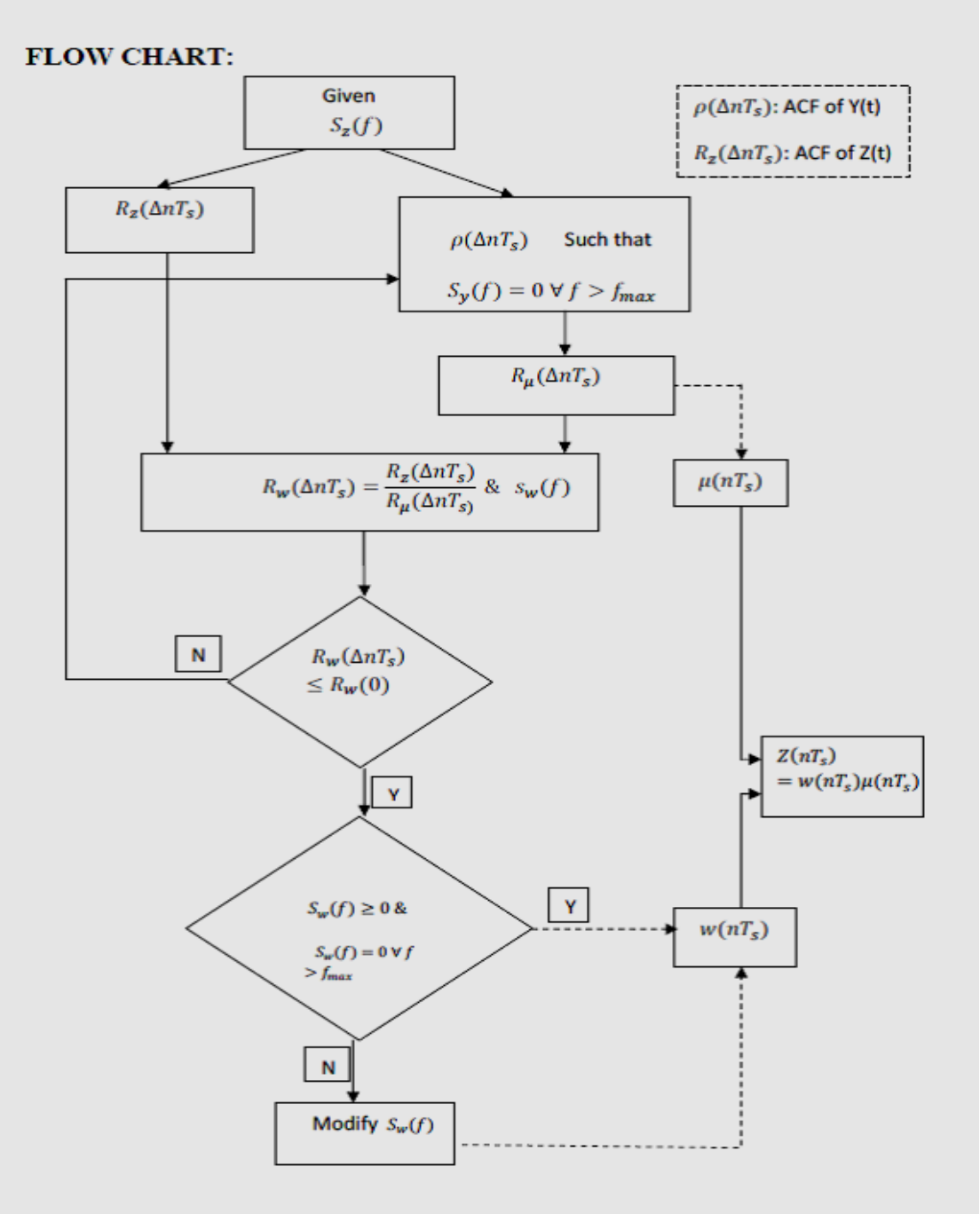

Figure 5.1: Flow chart of simulation process

5.1.1 Details of parameters, schemes and values used

- Software used: MATLAB R2007b(7.5)
- Simulated channel: Nakagami-*m* for $0.5 \leq m < 1$
- Number of bins: 200
- Number of frames: 1000

5.2 Results and Analysis

Fig 5.2.1: Nakagami-*m* envelop PDF for *m*=1, Ω=1

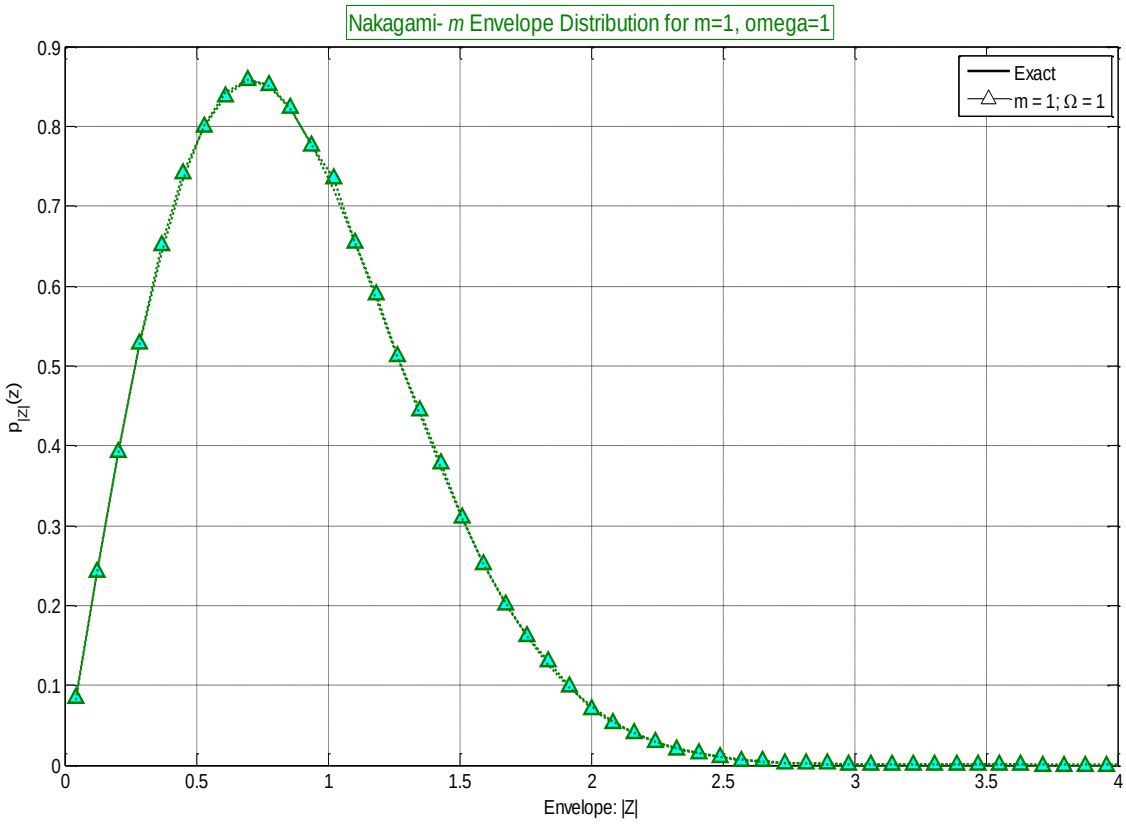

Comment: From this figure, as already discussed, the nakagami PDF is just same as that of Rayleigh PDF for the case of *m*=1. The plot also shows that the simulation result is exactly matched with the required one.

Fig 5.2.2: Nakagami-*m* envelope PDF for m=0.8, Ω=1

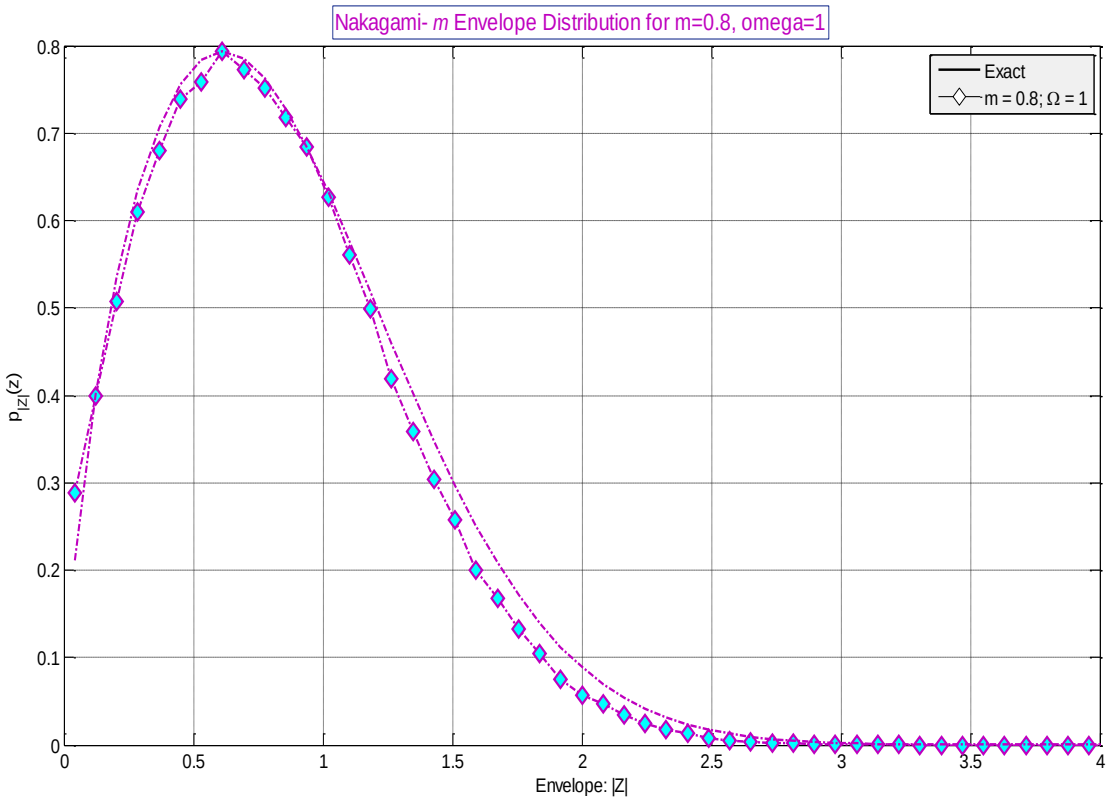

Fig: 5.2.3 Nakagami-*m* envelope PDF for *m*=0.8, Ω=1

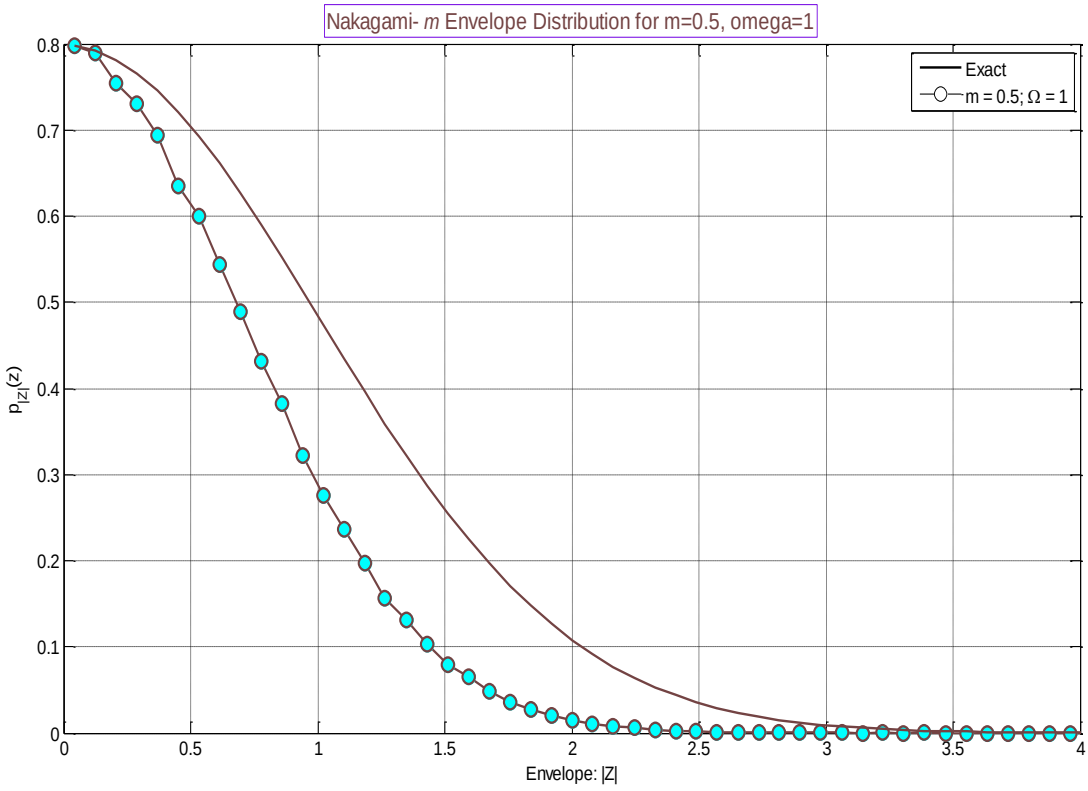

Comment: From this figure, as said earlier, the Nakagami-*m* PDF fallows the one sided Gaussian PDF for the case of *m*=0.5. The simulated results approximate the required results in this case.

Fig 5.2.4: Comparison of Nakagami-*m* envelope PDFs for *m*=0.5, 0.8 &1, Ω=1

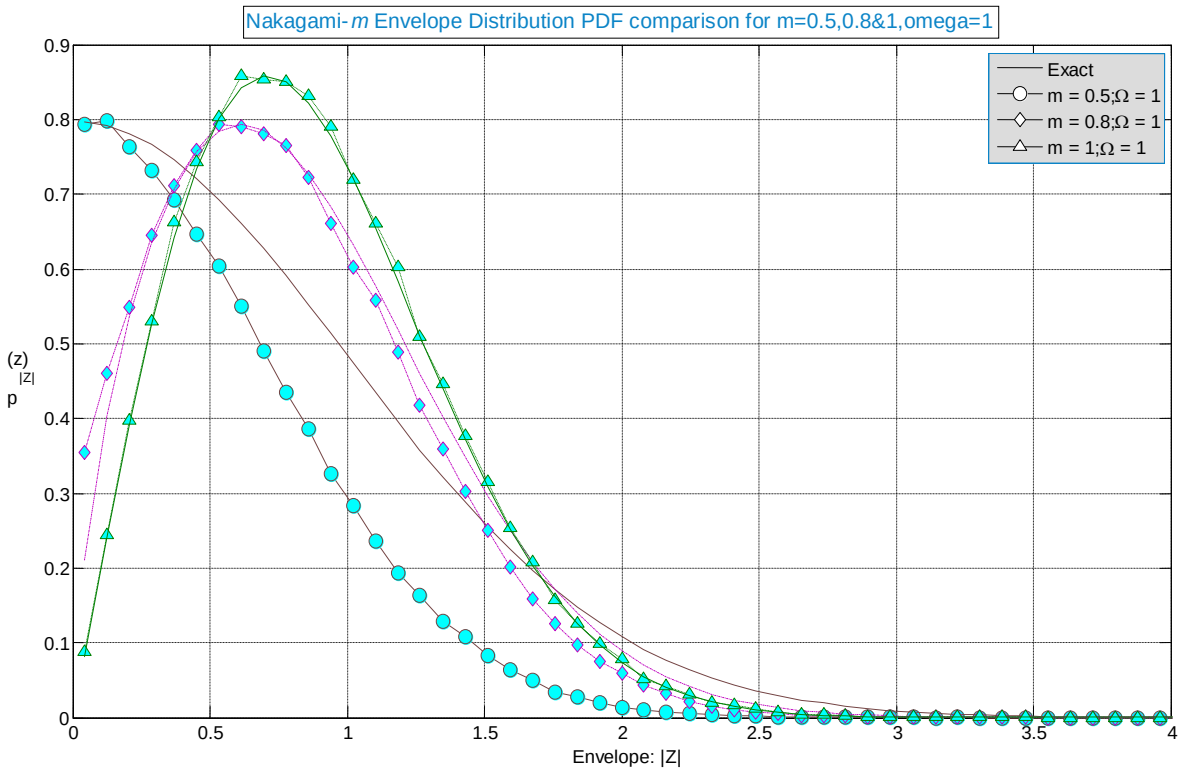

Comment: This plot showing how the PDF shape is changing for different values of *m*- parameter. It is clear that for the case of *m*=0.5, most of the multi path components are having zero amplitudes.

Fig 5.2.5: Nakagami-*m* phase PDF for *m*=1, Ω=1

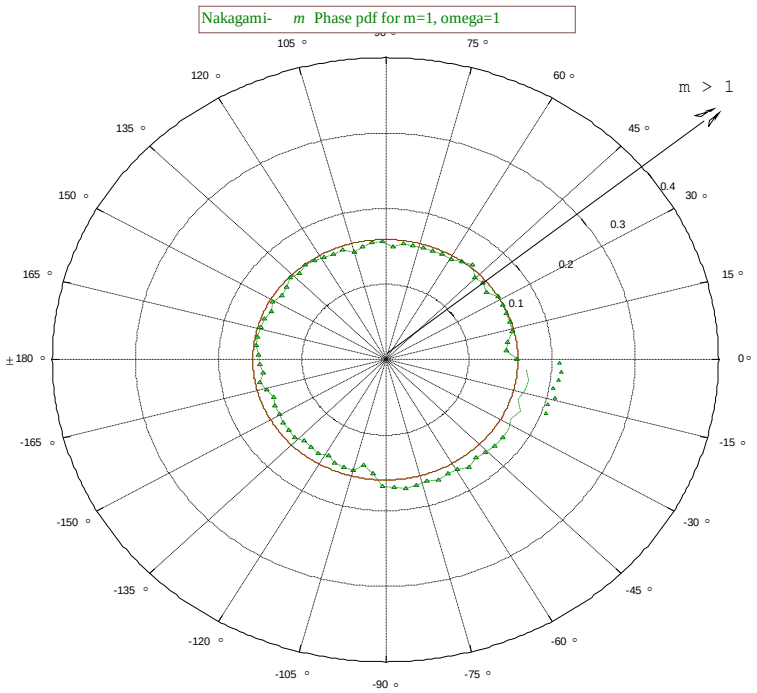

Fig 5.2.6: Nakagami-*m* phase PDF for *m*=0.8, Ω=1

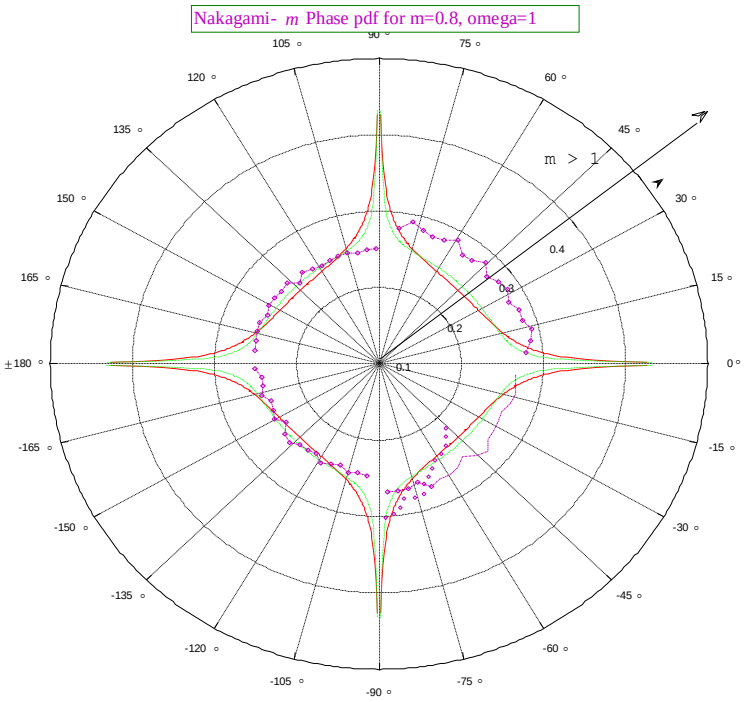

Fig 5.2.7: Nakagami-*m* envelope PDF for *m*=0.5, Ω=1

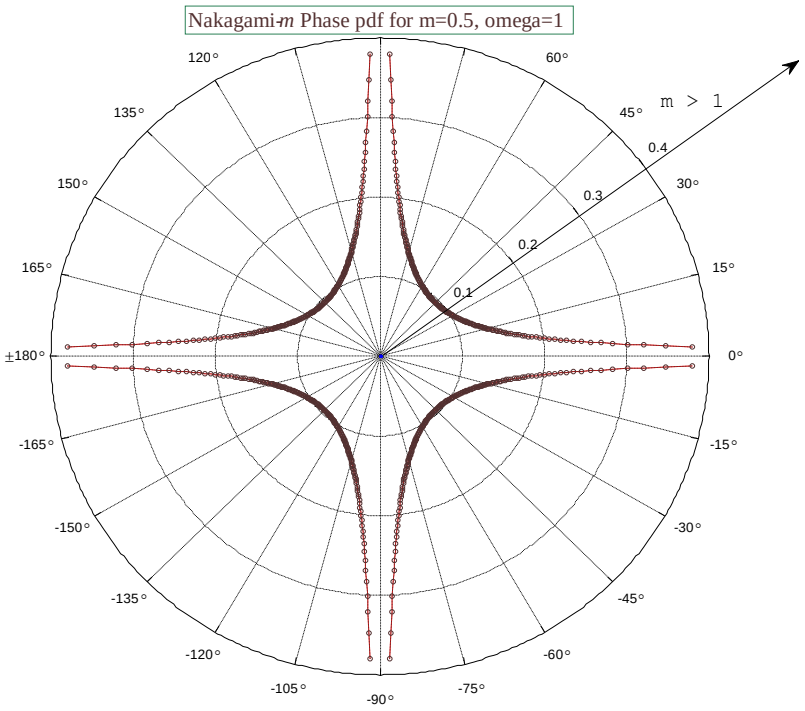

Fig 5.2.8: Comparison of Nakagami-*m* phase PDFs for *m*=0.5, 0.8 &1, Ω=1

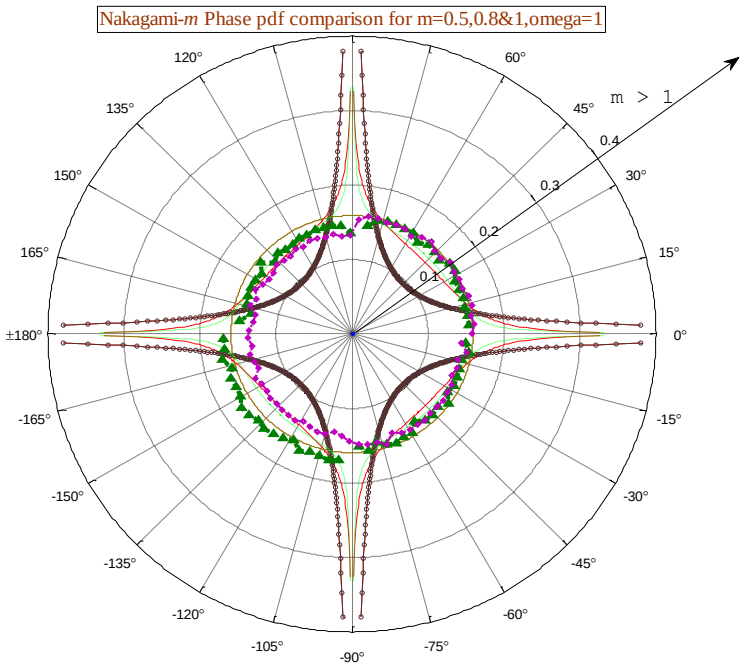

Comment: From the figures 5.2.5-8 for different values of m, we can conclude that the phase PDF is uniformly distributed within the interval [0 2π] except for the case of *m*=0.5 (one sided Gaussian). In the case of *m*=0.5, we can understand that most of the multi path components reach the receiver either straight or perpendicular to the receiving antenna.

Fig 5.2.9: Simulated Nakagami-*m* random process for *m*=1, Ω=1

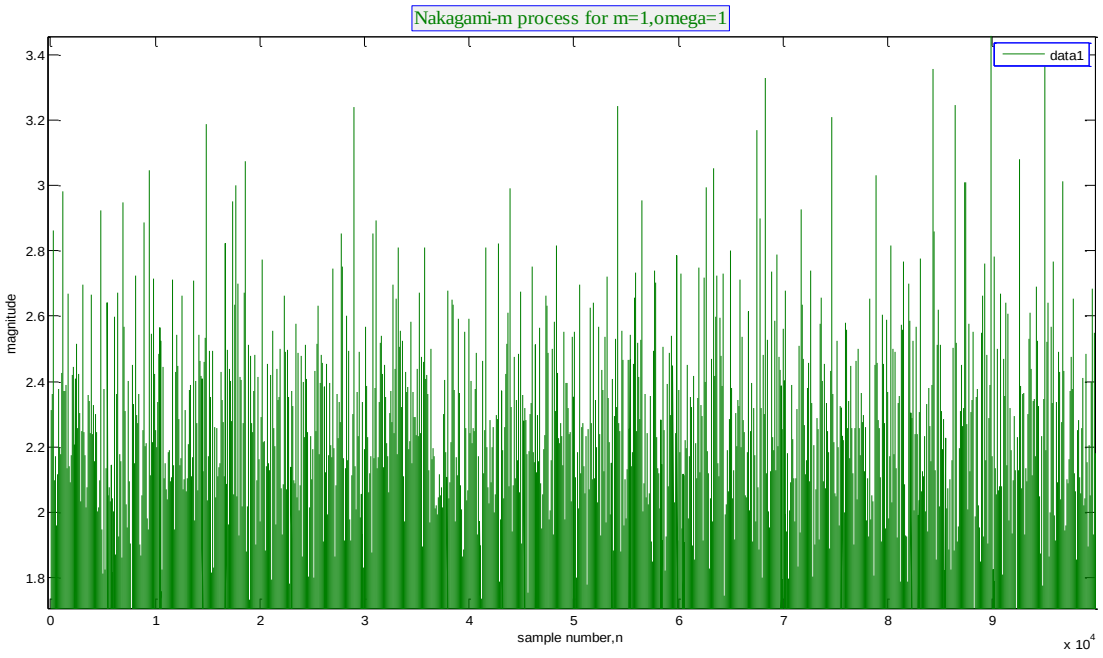

Fig 5.2.10: Simulated Nakagami-*m* random process for *m*=0.8, Ω=1

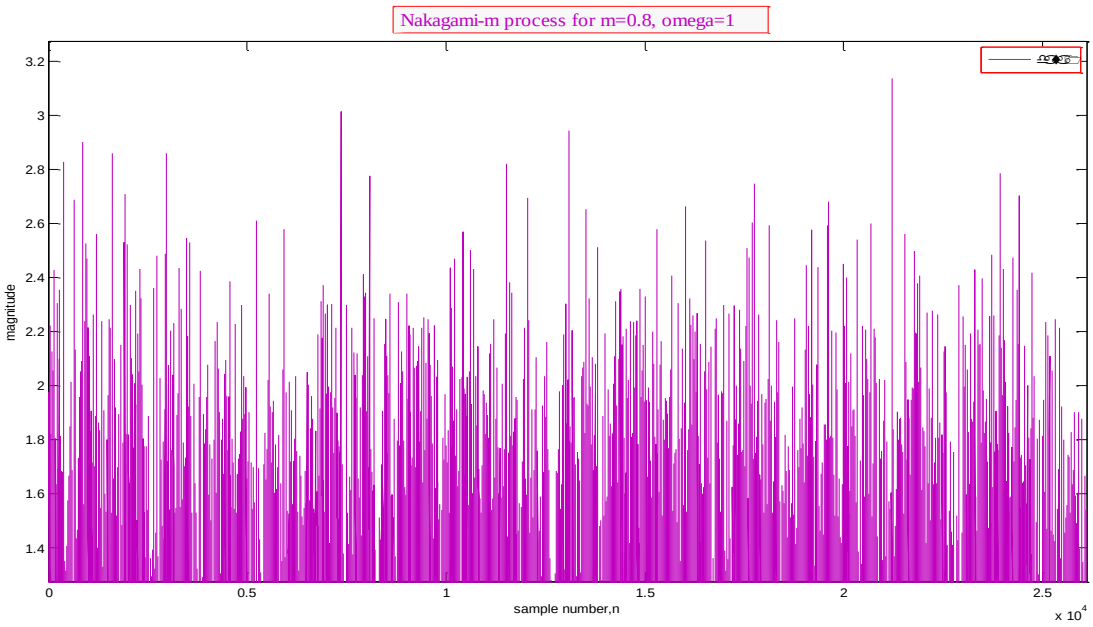

Fig 5.2.11: Simulated Nakagami-*m* random process for *m*=0.5, Ω=1

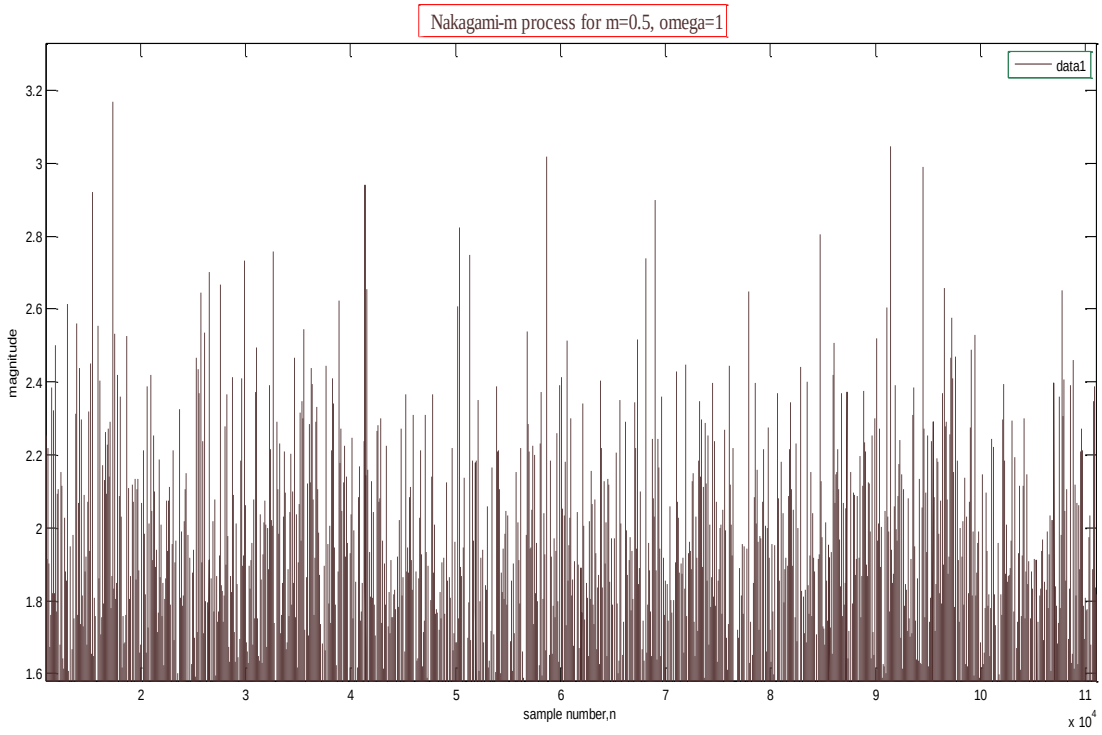

Comment: Figures 5.2.9-11 shows the simulated nakagami-m processes for different values of shaping parameter *m*.

Fig 5.2.12: Auto Correlation Function of the nakagami-m distribution for m=1

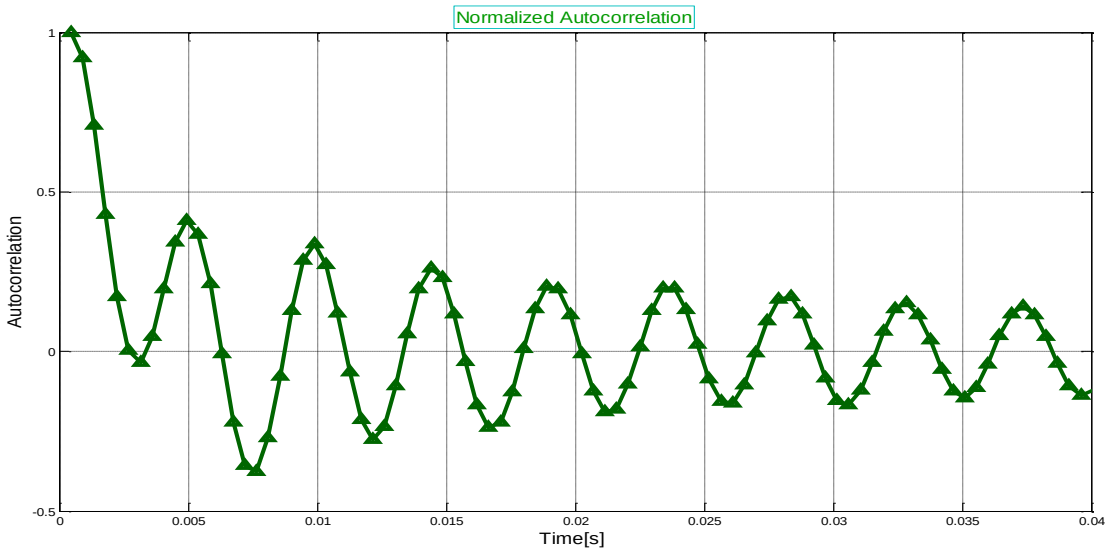

Comment: The autocorrelation function is looks like the sampling function due to the fact that PSD of the Rayleigh distribution is like a gate function.

Fig 5.2.13: Comparison of Nakagami-*m* envelope PDF s for *m*=1, Ω=1, 5& 10

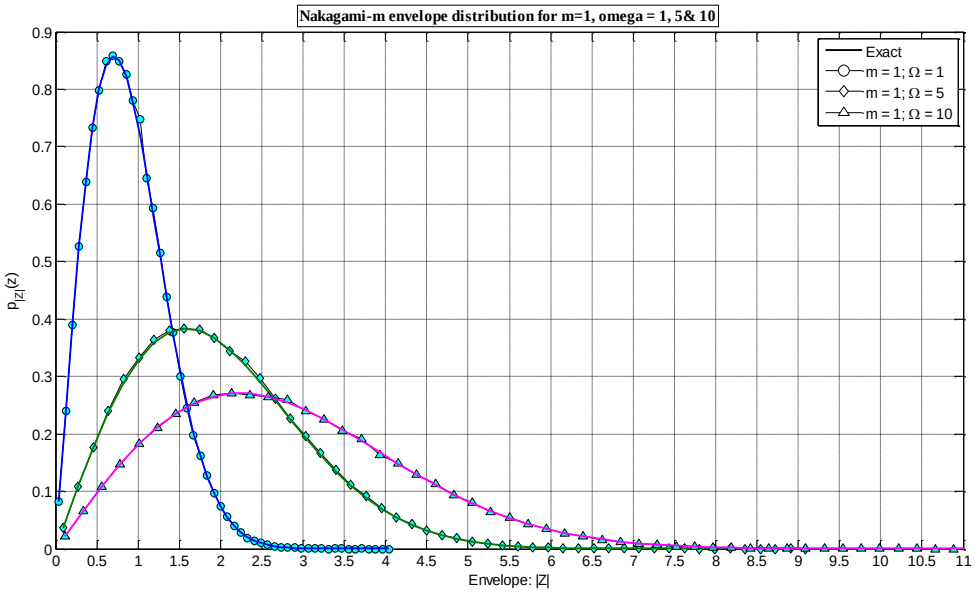

Comment: This figure shows how the Nakagami-*m* PDF changes its variance with the spreading parameter Ω for a single value of shaping parameter-*m*.

CHAPTER6

CONCLUSION AND FUTURE SCOPE

6.1 Conclusion

In this thesis report, a technique has been implemented as the multiplication of 2 stochastic processes to simulate Nakagami-*m* fading channel.

Firstly, complex Gaussian random process was generated with the help of rice's sum of sinusoids. Next, square root beta process was generated as the non linear transformation of the standard Normal random variates. The procedures are dictated to realize those 2 random processes.

The technique proposed here to model the nakagami-*m* fading channel for $0.5 \leq m < 1$ yields better results compared to the existing methods suggested by [8], [9]. In fact, the problems encountered in the simulation for generating Nakagami process as suggested by [8], [9] are bypassed with a special technique as suggested by [1] in this work.

The simulation results shown that PDF plots of the magnitude and phase are approximated the Nakagami-*m* and uniform distributions respectively. The power spectral density is the frequency domain dual of the autocorrelation function which is helpful to estimate the total power present in a random process.

The channel simulated here can be useful for the performance comparison, like bit error rate (BER), signal to noise ratio (SNR), of different m-ary modulation schemes such as QPSK, PSK, OFDM… under different fading channels.

6.2 Future scope

The technique implemented here, successfully, to simulate uncorrelated channels can also applicable to generate correlated channels also. The procedure is already given in this report itself.

By using any of the mathematical tools like MATLAB, the correlated channels can be readily implement which gives practical applicability of this method for the most common situation occurred in mobile communications.

Depending on the correlation between the channels, it is easy to find a better diversity technique which is suitable for mobile receivers.

REFERENCES

[1] Kun-Wah Yip, Tung-Sang Ng*,"* A Simulation Model for Nakagami-m Fading Channels, 0.5 < m < 1", *IEEE Trans. Commun.,* Vol. 48, pp.214-221, Feb. 2000.

[2] M. Nakagami, "Them-distribution—A general formula of intensity distribution of rapid fading," in *Statistical Methods of Radio Wave Propagation*, W. C. Hoffman, Ed. Oxford, U.K.: Pergamon, 1960, pp. 3–36.

[3] P. Hoeher, "A statistical discrete-time model for the WSSUS multipath channel," *IEEE Trans. Veh. Technol.*, vol. 41, pp. 461–468, Nov. 1992.

[4] P. M. Crespo and J. Jiménez, "Computer simulation of radio channels using a harmonic decomposition technique," *IEEE Trans. Veh. Technol.*, vol. 44, pp. 414–419, Aug. 1995.

[5] Theodore S. Rappaport, *Wireless Communications-Principles And Practice*, 2nd Ed. Prentice Hall, 2000.

[6] A. Papoulis, *Probabilities, Random Variables, and Stochastic Processes*, 4th ed. New York: McGraw-Hill, 2002.

[7] J. F. Mastrangelo, J. J. Lemmon, L. E. Vogler, J. A. Hoffmeyer, L. E. Pratt, and C. J. Behm, "A new wideband high frequency channel simulation system," *IEEE Trans. Commun.*, vol. 45, pp. 26–34, Jan. 1997.

[8] M. Pätzold, U. Killat, F. Laue, and Y. Li, "On the statistical properties of deterministic simulation models for mobile fading channels," *IEEETrans. Veh. Technol.*, vol. 47, pp. 254–269, Feb. 1998.

[9] H. Kong and E. Shwedyk, "A hidden Markov model (HMM)-based MAP receiver for Nakagami fading channels," in *Proc. 1995 IEEE Int. Symp. Information Theory*, Whistler, BC, Canada, Sept. 17–22, 1995, pp. 210.

[10] W. R. Braun and U. Dersch, "A physical mobile radio channel model," *IEEE Trans. Veh. Technol.*, vol. 40, pp. 472–482, May 1991.

[11] U. Dersch and R. J. Rüegg, "Simulation of the time and frequency selective outdoor mobile radio channel," *IEEE Trans. Veh. Technol.*, vol. 42, pp. 338–344, Aug. 1993.

[12] N.L. Johnson, S. Kotz, and N. Balakrishnan, *Continuous Univariate Distributions*, 2nd ed. New York: Wiley, 1995, vol. 2.

[13] M. Grigoriu, *Applied Non-Gaussian Processes*. Englewood Cliffs, NJ: Prentice-Hall, 1995.

[14] M. Patzold, *Mobile fading channels-modeling, analysis& synthesis*, Wiley, 2002.

[15] Q. T. Zhang, A Decomposition technique for efficient generation of correlated Nakagami Fading Channels.

[16] Y. Chen and N. C. Beaulieu, "Estimation of Rician and Nakagami distribution parameters using noisy samples," IEEE Int. Conf. on Commun. (ICC), June 2004.

[17] C. Tepedelenlioglu and G. Ping, "Practical issues in the estimation of Nakagami-m parameter," Proc. IEEE GLOBECOM, vol. 2, pp. 972–976, 2003.

[18] J. Cheng and N. C. Beaulieu, "Generalized moment estimators for the Nakagami fading parameter," IEEE Commun. Lett. Vol. 6, pp. 144–146, Apr. 2002.

[19] Lingzhi Cao; Beaulieu, N.C.; "A simple efficient procedure for generating bivariate Nakagami-m fading samples" Communications, 2005. ICC 2005. 2005 IEEE International Conference on Commun. Volume 2, 16-20 May 2005 Page(s): 886 - 889 Vol. 2.

[20] R. B. Ertel and J. H. Reed, "Generation of correlated Rayleigh fading envelopes" IEEE commun. lett. Vol. 3 pp, 276-278, Oct 1998.

[21] Zhang Q. T. "Correlated Nakagami Fading Channels with different fading parameters: A generic characterization with Application," Communications, 2002. ICC 2002. IEEE International Conference on Volume 2, 28 April-2 May 2002 Page(s): 704 - 708 vol.2.

[22] Norman C. Beaulieu and C. Cheng, "Efficient Nakagami- m Fading Channel Simulation," IEEE trans. on vehicular Tech. vol.54 no.2, pp. 413-424 March 2005.

[23] Tsan-Ming Wu, Shiuna-Yuan Tzeng, "Sum-of-sinusoids based simulator for Nakagami-m fading channels" Vehicular Tech. Conf. 2003, VTC 2003-Fall IEEE 58th vol. 1, 6-9 Oct 2003 Page(s): 158-162.

[24] Yacoub, M.D.; Bautistu, J.E.V.; Guerra de Rezende Guedes, L.; "On higher order statistics of the Nakagami-m distribution" Vehicular Technology, IEEE Transactions Volume 48, Issue 3, May 1999 Page(s): 790 – 794.

[25] Iskander, C.D.; Takis Mathiopoulos, P., "Analytical level crossing rates and average fade durations for diversity techniques in Nakagami fading channels," Communications, IEEE Transactions on Volume 50, Issue 8, Aug. 2002 Page(s): 1301 – 1309.

[26] Merilee Ford, H. Kim Lew, Steve Spanier, and Tim Stevenson, *Internetworking Technologies Handbook*, 4th Ed. Cisco press, 2003.

[27] http://philsci-archive.pitt.edu/archive/00002412/01/Simulations.pdf

[28] Andrea goldsmith, *Wireless Communications*, Cambridge University Press, 2005.